Università degli Studi di Ferrara

DOTTORATO DI RICERCA IN
BIOCHIMICA, BIOLOGIA MOLECOLARE E BIOTECNOLOGIE

CICLO XXI

COORDINATORE Prof. FRANCESCO BERNARDI

CHARACTERIZATION OF THE MECHANISM OF 6-PHOSPHOGLUCONATE DEHYDROGENASE FROM *TRYPANOSOMA BRUCEI* AND ITS INTERACTION WITH INHIBITORS BY ISOTHERMAL TITRATION CALORIMETRY

Settore Scientifico Disciplinare BIO/10

Dottorando
Dott. Montin Katy

Tutore
Prof. Dallocchio Franco

Anni 2006/2008

INDEX

PART I RESULTS AND DISCUSSION

PART II

INTRODUCTION

Human African Trypanosomiasis (HAT), or sleeping sickness, is caused by infection with parasitic protozoa of the *Trypanosoma brucei* (*T. brucei*) subspecies, which are introduced to the human bloodstream by the bite of infected tsetse flies in the inter-tropical regions of Africa. *Trypanosoma brucei gambiense*, found in West and Central Africa, leads to a chronic form of the disease. *T. b. rhodesiense*, found in East Africa, leads to a more virulent and acute condition. Once parasites establish within the cerebrospinal fluid death is an inevitable consequence of infection unless the disease is treated. Sleeping sickness is a re-emerging infectious disease with the number of infected individuals presently estimated at more than 300.000 [1], and about 55 million people are at risk of infection. No vaccines exist against sleeping sickness, and the prospects of prophylactic immunisation are poor since the parasites change their surface coat periodically in a process known as antigenic variation [2]. Drugs remain the principal means of intervention. Four drugs are currently registered [3]. The drug of choice depends on whether the disease is diagnosed before parasites have established within the cerebrospinal fluid. Problems associated with the current therapies of sleeping sickness include toxicity, resistance and lack of a guaranteed supply [4].

Drug target

New drugs are urgently needed for human African trypanosomiasis. Moreover, as the emergence of resistance is likely to be an ongoing problem, a system should be established to ensure new products become available on a relative frequent basis. In order to act, drugs must specifically inhibit a target within the parasite. Trypanosomes diverged early in the eukaryotic lineage [5], and their biochemical constitution differs in many respects from that of mammalian cells. Pathways present

in trypanosomes, but absent from mammalian hosts, may provide selective targets. Systematic sequencing of pathogen genomes is now possible. A natural progression from comparative biochemistry has been to proceed to trypanosomatid genome sequencing projects to identify new drug target. Trypanothione and its metabolism, glucose metabolism and its unusual compartmentalisation within peroxisome-like organelles called glycosomes, purine metabolism, lipid biochemistry and polyamine metabolism have all been proposed as good targets [6].

The gene knockout approach [7] is now widely used to provide evidence on whether a gene is essential, and thus a credible target for inhibitory drugs. The discovery that RNA interference, a phenomenon whereby double stranded RNA molecules lead to suppression of expression of the genes from which they are derived, [8] has led to the development of simple techniques enabling inducible suppression of gene expression in these parasites. This has offered an accelerated route to loss of gene function and is now enhancing the rate at which gene products can be validated as drug targets.

Proteins like trypanothione reductase, that are unique to trypanosomes, have been proposed as ideal targets [9]. However other enzymes, which are present in both host and parasite, can also be effective drug target. Indeed ornithine decarboxylase, present in both host and parasite, is the only known target for any registered drug used against trypanosomatids, being inhibited by eflornithine (DFMO).

Other enzymes found in both mammalian cells and trypanosomatids can also be good drug targets because they have structural peculiarities that can be targeted by selective inhibitors. This has been clearly demonstrated in the case of the key glycolytic enzyme glyceraldehydes-3-phosphate dehydrogenase (GAPDH). Differences in the coenzyme (NAD^+) binding site were identified using comparative X-ray crystallographic analysis [10]. Structures based on adenosine, as analogues of co-factor, were shown to selectively inhibit the trypanosomatid enzymes and also to kill both *T. brucei* and *T. cruzi*.

The pentose phosphate pathway (PPP) (Fig.1) is another key pathway of glucose metabolism present in most species [11]. . The pathway is developmentally regulated

in *T. brucei*, with all enzymes of the PPP present in the procyclic form and the oxidative branch enzymes in the bloodstream form [12]. We have been engaged in studies on 6-phosphogluconate dehydrogenase, the third enzyme of this pathway. The trypanosomal version differs significantly in sequence when compared to its mammalian counterpart and is a validated target for therapy [46].

The dehydrogenases of the pentose phosphate pathway (PPP), glucose-6-phosphate dehydrogenase (G6PD) and 6-phosphogluconate dehydrogenase (6PGDH), are $NADP^+$ dependent in most organisms. The pathway has two main parts: an oxidative branch and a non-oxidative, rearrangement branch. The major functions of the pathway are the generation of the reduced coenzyme NADPH and the production of ribose 5-phosphate for nucleotide and nucleic acid synthesis. NADPH is essential in protecting the organism against oxidative stress and is required for a variety of reductive biosynthetic reactions, particularly lipid production. The whole of the PPP operates in mammals. The first enzyme of the pathway, G6PDH has been shown to be essential for defence against oxidative stress in humans [68]. Serious G6PDH deficiency is well known and results in haemolytic anaemia.

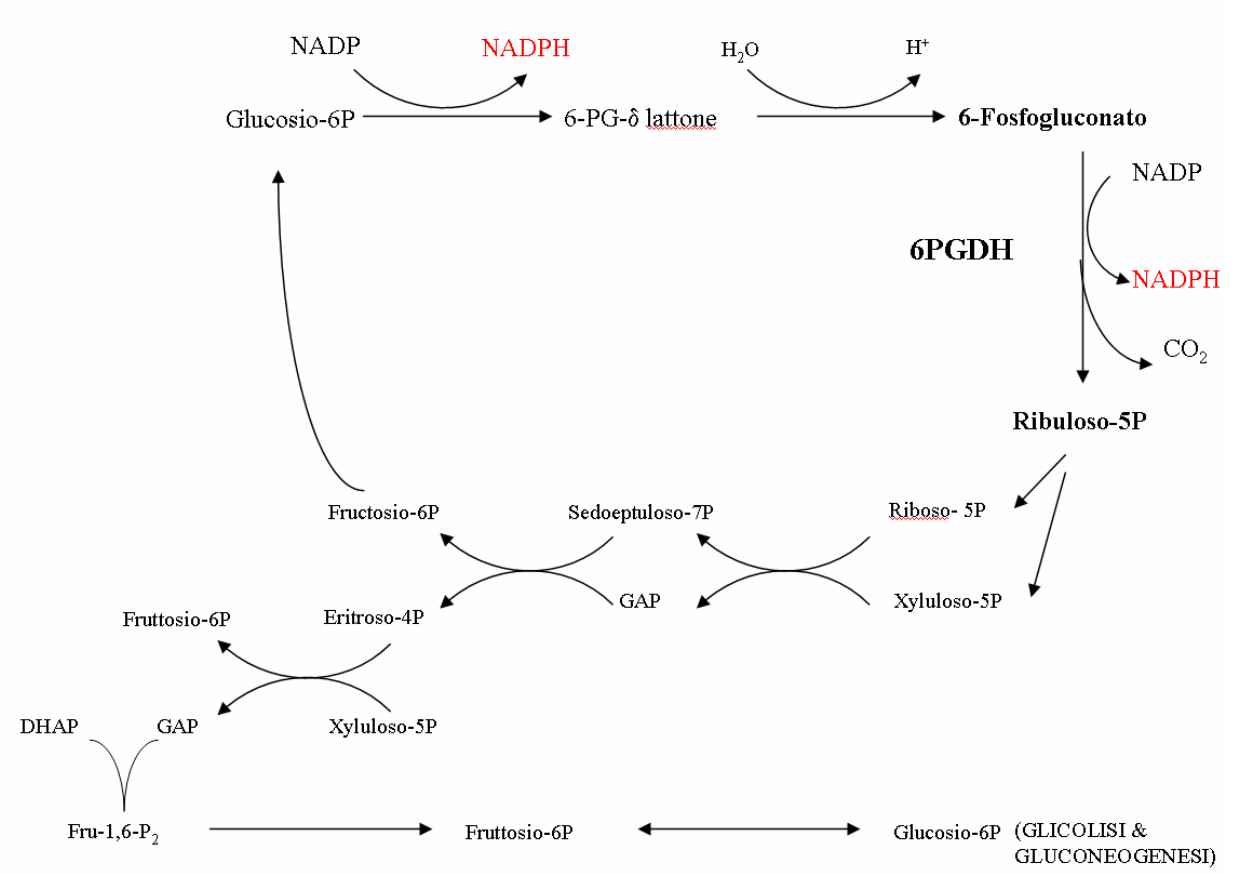

Fig.1. Pentose Phosphate Pathway

Action mechanism of 6-phosphogluconate dehydrogenase

6PGDH is the third enzyme of the Pentose Phosphate Pathway (Fig. 1), which provides both NADPH, required for many biosynthetic and detoxification reactions, and also active in protection against oxidative stress, and ribose, essential for nucleotide biosynthesis.

It catalyses the $NADP^+$-dependent oxidative decarboxylation of 6-phospho-D-gluconate (6PG) to D-ribulose 5-phosphate (Ru5P), *via* 3-keto 6PG and a probable 1, 2-enediol as intermediates (Fig. 2) **[**13,14**]**.

Two residues, one acting as an acid and the other as a base are postulated to assist all the three catalytic steps of the reaction: dehydrogenation, decarboxylation and keto-enol tautomerization. These residues, which in the *T. brucei* enzyme are Glu-192 and Lys-185, have been identified on the basis of crystallographic evidence and site-directed mutagenesis [15-17]. The lysine residue is thought to be protonated in the free enzyme and unprotonated in the enzyme-substrate complex, where it has to receive a proton from the 3-OH of 6PG as a hydride is transferred from C-3 of 6PG to NADP (Fig.2). The resulting 3-keto-6PG intermediate is then decarboxylated to form the enediol of 5-phospho-ribulose. At this stage an acid, which is thought to be the same Lys-185, is required to donate a proton to the C-3 carbonyl group of the keto-intermediate to facilitate decarboxylation. Both a base and an acid are needed in the tautomerisation of the enediol intermediate to yield the ketone ribulose 5-phosphate product, with the acid (Glu-192) required to donate a proton to the C-1 of the enediol intermediate and the base (the same Lys-185) accepting a proton from its 2-hydroxyl (Fig.2, Fig.3). At the end of the reaction the protonation state of the two catalytic groups is the opposite to that at the beginning of the reaction; thus an intramolecular proton transfer is required for another cycle of enzyme activity.

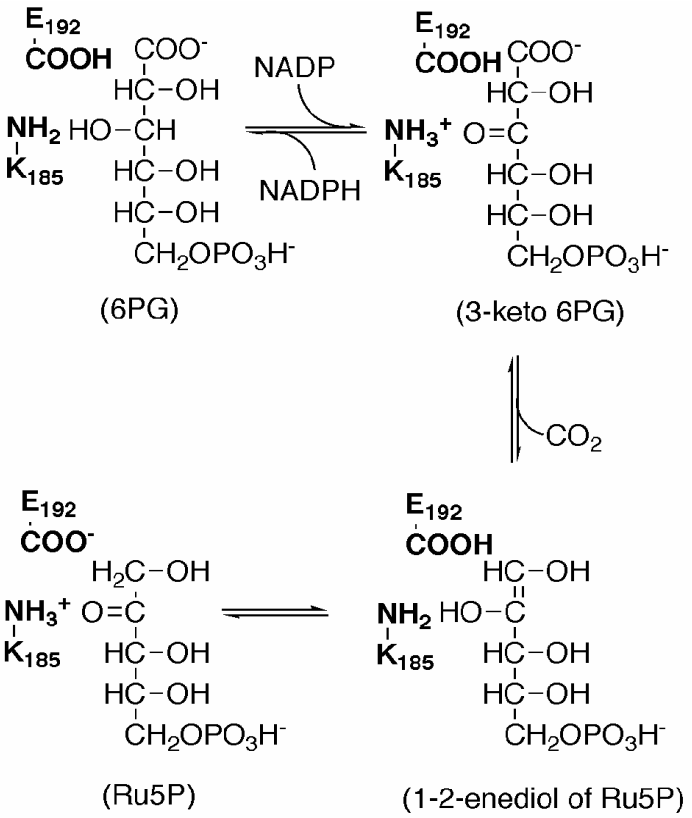

Fig. 2. 6PGDH-catalysed reaction and the two main amino acid residues involved.

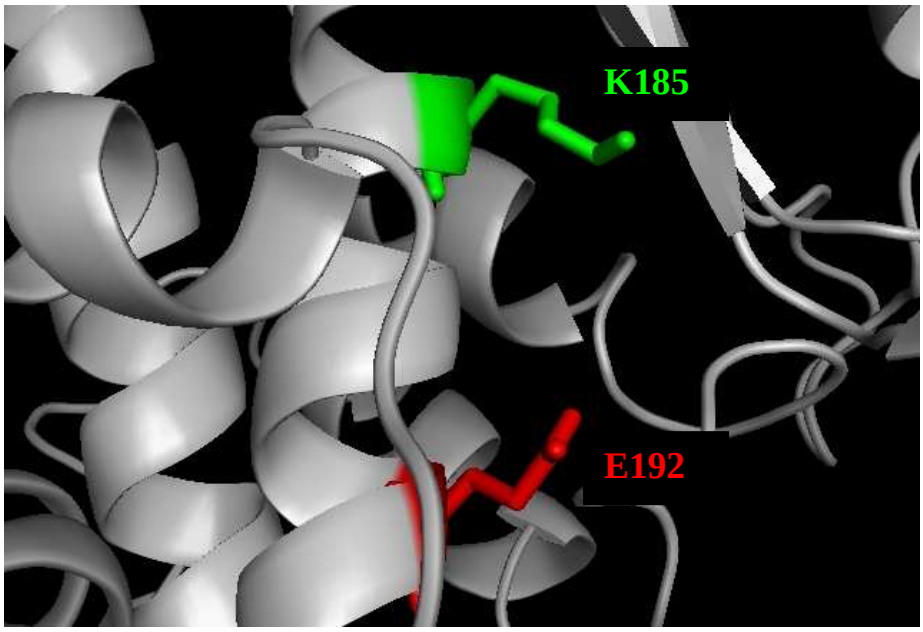

Fig.3. *T. brucei* 6PGDH active site with the position of the two residues, discussed in the introduction.

Structure of 6PGDH

The 6PGDH is a homodimer with subunit size 50kDa. The 6PGDH of *T. brucei* shows only a 33% amino acid identity with the mammalian 6PGDH [18]. Identity is higher (37.3%) with both the chloroplast and the cytosolic 6PGDH from spinach [19]. This may reflect the evolutionary history of the Kinetoplastida, the phylogenetic order to which trypanosomes belong, which have been proposed to have derived from an ancestor common with the primitive plants Euglenoid algae [20]. A number of genes in trypanosomes appear to relate more closely to those of cyanobacteria and plastids as well as algal and other plant genes than to those of other eukaryotic lineages [20]. The sequence of 6PGDH from 9 different species, *Saccharomyces cerevisiae*, *Drosophila melanogaster*, *Homo sapiens*, sheep, *Escherichia coli*, *Lactococcus lactis, Plasmodium vivax, Trypanosoma brucei e Leishmania major*, have been aligned using the programs MultAlin [21] e ESPript [22] to show the conserved amino-acids among species. Of the 482 amino-acids that belong to one subunit, 88 are conserved in all species (Fig. 4)[23].

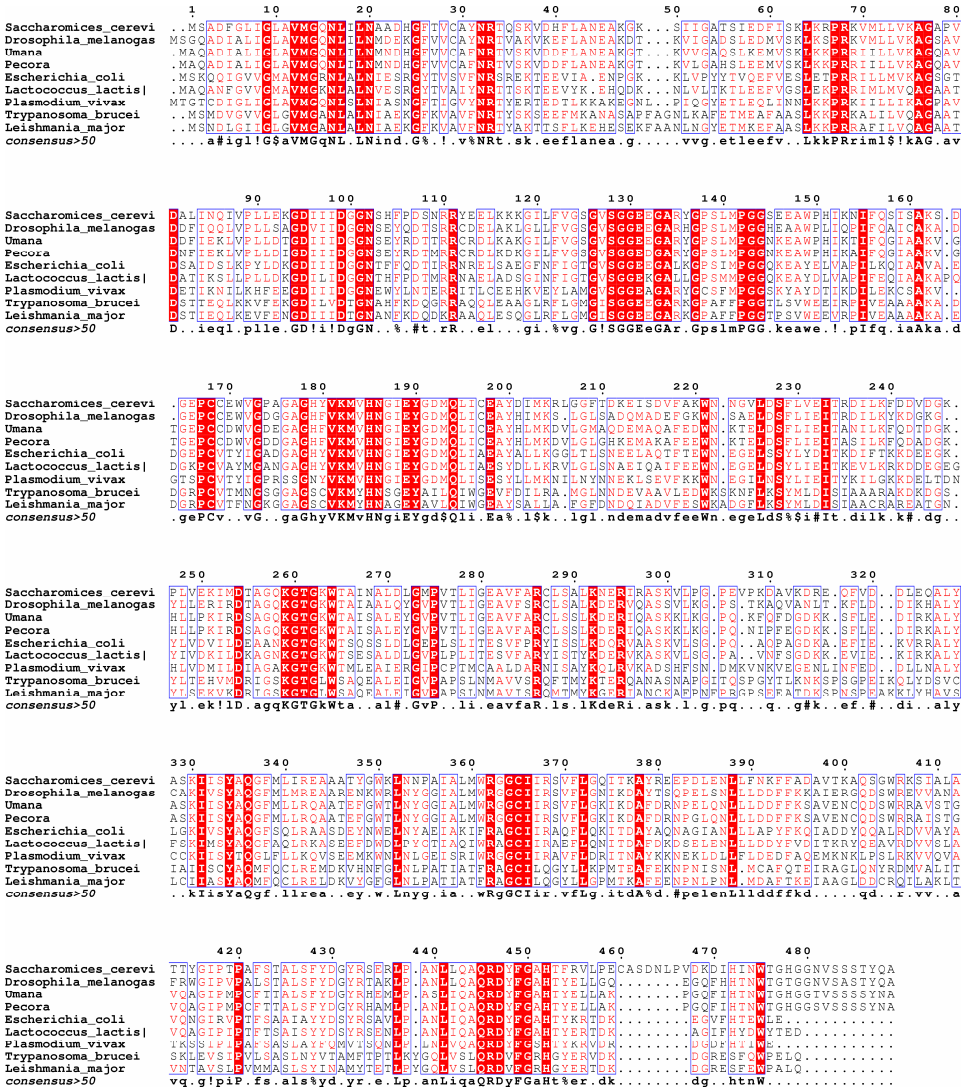

Fig. 4. Multiple alignment of 6PGDH from several species.

The 3-dimensional structure of the *T. brucei* 6-phosphogluconate dehydrogenase has been solved at 2.8 Å resolution (Fig. 5)[24]. The sheep liver enzyme, which has 97% sequence identity to the human enzyme, has been described at 2 Å [25] resolution and enzyme-coenzyme and enzyme-substrate complexes have been reported at 2.3 Å -2.5 Å resolution [26].

The structure of *Lactococcus lactis* 6PGDH in ternary complex with NADP and the product Ru5P or the inhibitor 4-phospho-D-erythronohydroxamic acid (PEX) were also reported [27].

The *T. brucei* monomer

The 6PGDH monomer has three domains (Fig.5).

The N- terminal “coenzyme” domain (residues 1-178) contains a typical dinucleotide binding Rossmann fold (1-130, βA ….βF with intervening helices) and a further α−β−α unit (132-161, αf-βG-αg) with the strand βG antiparallel to the first 6 strands. The coenzyme binding site is at the carboxyl ends of the strands of the parallel sheet, with the two ribose moieties and the bis-phosphate straddling the sheet. The dinucleotide binding fingerprint, at the tight turn following βA, is GxGxxG in the *T. brucei* enzyme while in the ovine enzyme it is GxAxxG as in almost all known 6PGDHs. As the two subunits of the *T. brucei* dimer were not crystallographically equivalent, slightly different conformations of two loops in the coenzyme domain could be seen [15]. Crystallographic symmetry precludes such observations in the sheep liver enzyme [24]. The second all “helix” domain (179-441, αh…αr) forms one part of the dimer interface and the “tail” (442-478, αs…C terminus) penetrates the second subunit (Fig. 6).

The substrate site lies at the interface between the helical domain and the coenzyme binding domain of one subunit and the tail of the second; residues which bind 6PG come from all three domains.

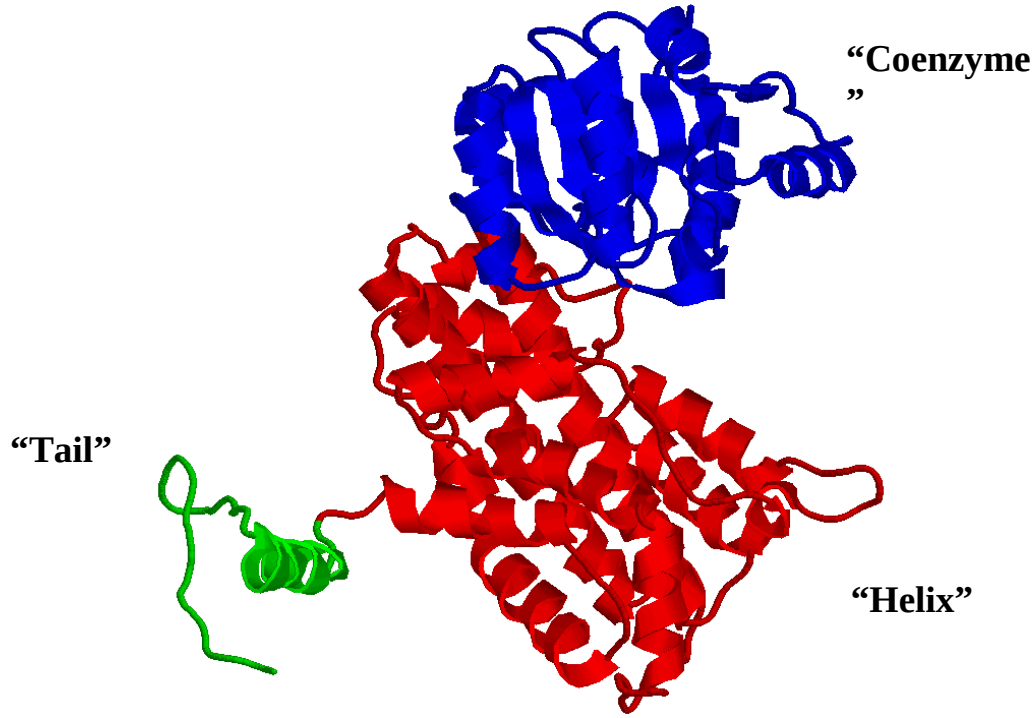

Fig 5. Monomer of the *T. brucei* 6PGDH.

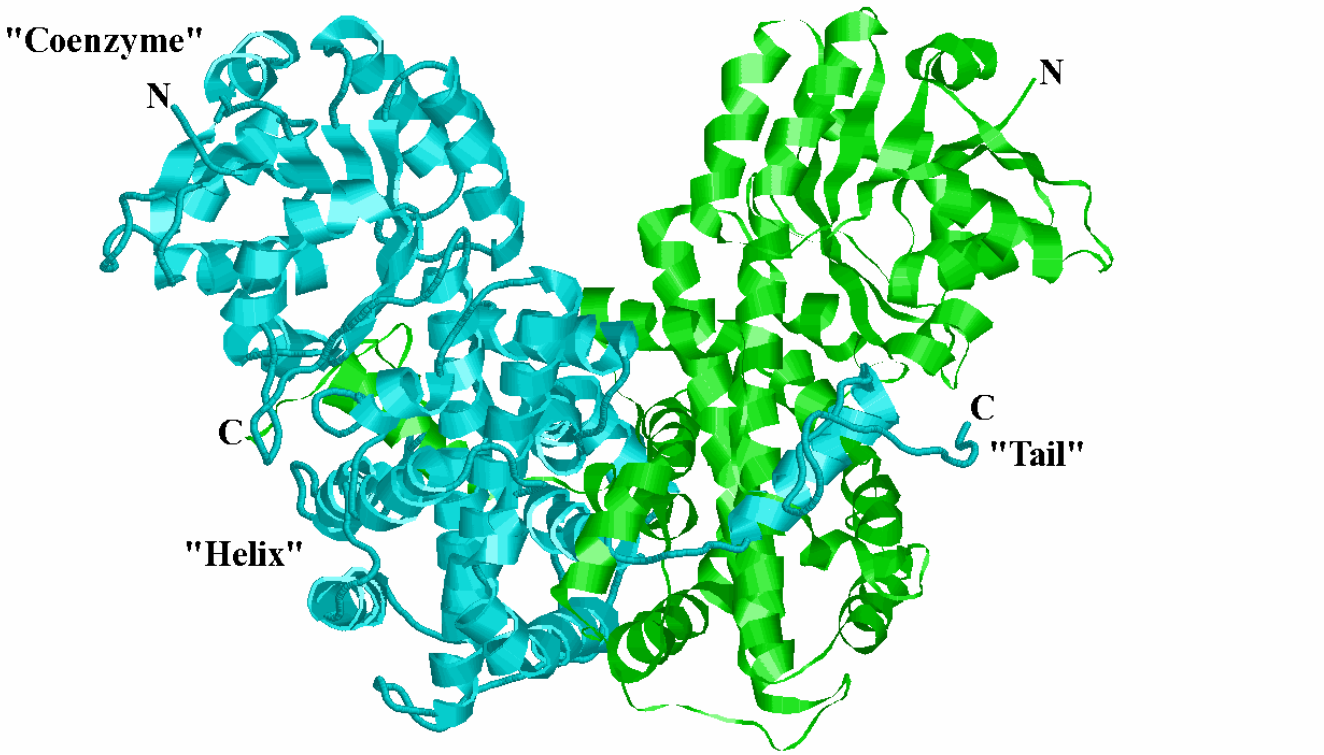

Fig. 6. Dimer of the *T. brucei* 6PGDH. The two subunits are drawn in blue and in green.

The dimer interface

The mode of dimerisation, with the tail of one subunit penetrating the other, is conserved between species. Although the dimer interface is structurally well conserved, with 106 of the 134 residues contributing to the interface of the parasite enzyme structurally equivalent to those in the sheep enzyme, only nine fully conserved residues have a major role in dimer formation. Three of these residues are part of the tail domain. The most significant difference in the nature of the interface is where the tail of one monomer threads through the other and contributes to the substrate binding site. The tail of the *T. brucei* enzyme is highly charged: 13 residues of 37 are aspartate, glutamate, histidine, lysine or arginine; the sheep enzyme has only seven charged residues in the longer (48 residues) tail. The significance of this is not yet certain but the profound distinctions at the interface may be amenable to drug targeting as techniques for disturbing protein interactions are developed.

Substrate binding site

Of the 19 residues within 4 Å of 6PG (Fig. 7): Asn 104 -102s (the sheep numbering is denoted by a lower case s), Ile 129 - Val 127s, Ser 130 - 128s, Gly 131 - 129s, Gly 132- 130s, Lys185 - 183s, His 188-186s, Asn 189 - 187s, Glu 192 - 190s, Tyr 193-191s, Ser 261- Gln 259s, Lys 262 -260s, Gly 263-261s, Thr 264- 262s, Arg 289-287s, Ile 373- 366s, Arg 453-446s, Phe 456- 449s, His 459- 452s, as bound in the sheep enzyme or modelled into the *T. brucei* enzyme, 14 are conserved for all species studied to date. Five of the substrate neighbours come from the coenzyme domain, eleven from the helical domain and three from the tail of the second subunit. The conserved lysine (Lys 183s, Lys 185) predicted to be the base in the reaction is on αh; the five residues in this helix, which interact with substrate, have moved less than 0.5 Å in the *T. brucei* 6PGDH compared to the sheep structure.

There are, however, several residues that are second nearest neighbours to the substrate and differ in the *T. brucei* enzyme from sheep. They include Thr 102 (Gly 100s), Ala 141 (Ser 139s), Phe 143 (Met 141s), Ser 190 (Gly 188s), Leu 196 (Met 194s), Leu 374 (Ile 367s), Ser 450 (Gln 443s and Ser only in *T. brucei*) and Arg 458 (Ala 451s and Arg only in *T. brucei*). The Nη 1 of Arg 446s (Arg 453) is a ligand to the 6-phosphate of 6-phosphogluconate. In the sheep enzyme Arg 446s is oriented by a hydrogen bond from its Nε to the Oε1 of Gln 443s (equivalent to Ser 450 in *T. brucei*), while Gln 443s Nε2 interacts with the carbonyl of Gly 258s (equivalent to Gly 260 in *T. brucei*). Residue 443s is therefore important in constraining the movement of Arg446s and defining the orientation of the phosphate of 6PG. In *T. brucei* 6PGDH, the hydroxyl of Ser 450 hydrogen bonds to the main-chain carboxyl oxygen of Arg 258, but there is no interaction with Arg 453.

Arg 458 interacts with the highly conserved Glu 133 (Glu 131s), which should have further implications for interaction with substrate since the carboxyl oxygens of 6PG interact with residues of the βF-αf turn (130- 132, 128s- 130s). These residues have moved almost 1 Å from their position in the sheep enzyme; the movement is correlated with the differing inter-domain hinge angles. Despite the conservation of first neighbours to 6PG, these changes provide means by which the affinity for substrate and substrate analogues may vary between species, and suggest possible targets for substrate analogue and potential drug interaction.

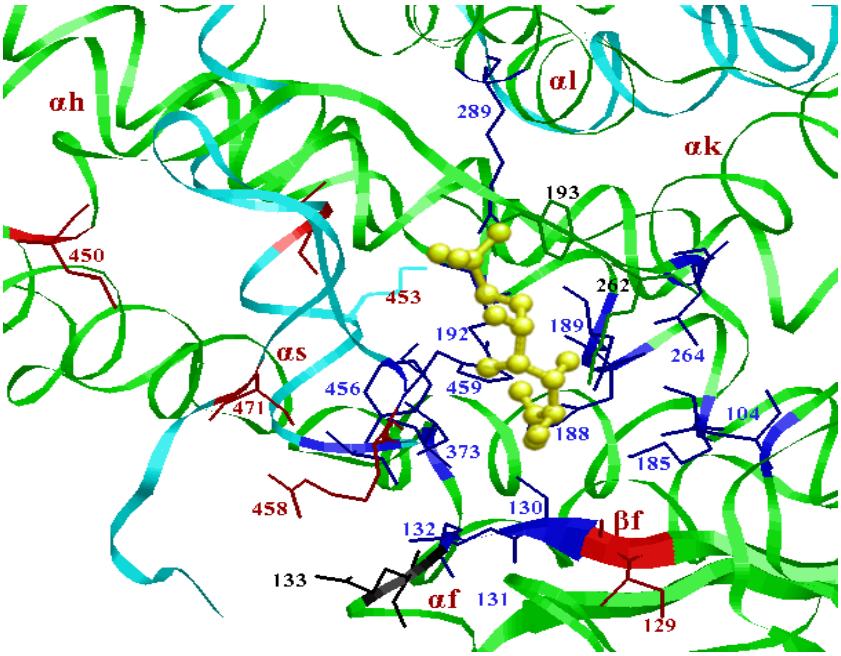

Fig. 7. Substrate binding site.

Coenzyme binding site

The equivalent folds of the *T. brucei* and sheep enzymes suggest that coenzyme binding will be similar although differences do exist, and the recent targeting of selective inhibitors to the NAD^+ binding domain of trypanosomatid GAPDH demonstrates how subtle differences in coenzyme binding may be exploited in selective drug design [10]. The coenzyme binding domain of 6PGDH has 70 residues identical in the sheep and *T. brucei* enzymes (Fig. 8). The oxidised coenzyme analogue 8-bromoadenine dinucleotide phosphate Nbr^8ADP^+, can be diffused into crystals of sheep 6PGDH apo-enzyme. It binds in a manner similar to that seen in many enzymes with the dinucleotide binding fold, with the adenine ribose approaching the βA-αa tight turn, the "coenzyme fingerprint". On binding the analogue, there is little main-chain movement: 0.25 Å for all main-chain atoms within 10 Å of the analogue [26]. Of the 17 residues of sheep 6PGDH, which are within 4 Å of the active oxidised coenzyme analogue, 12 are identical for the *T.*

brucei and sheep structures. The K_m for $NADP^+$ for *T. brucei* 6PGDH is 1 μM while that for sheep enzyme is several times higher ranging from 5.7-8.9 μM depending on pH and ionic strength [28]. Sequence differences at the coenzyme binding site may affect the affinity for $NADP^+$ between species.

The mean main-chain movement for the 17 residues of the sheep enzyme on binding the analogue is 0.31 Å; only Lys 75s moves significantly (0.77 Å). Hydrogen bond interaction of the sheep enzyme with oxidised coenzyme is predominantly that of the 2'-phosphate and adenine ribose to triplet Asn 32s, Arg 33s, Thr 34s directly following βB (Asn 31, Arg 32, Thr 33 in *T. brucei*).

The additional hydrogen bonds are to the nicotinamide amide function from a conserved methionine of the fingerprint (Met 13s) and from a glutamate of αf (Glu 131s) conserved in 68 of 70 species. All residues with side-chain hydrogen bonds are conserved between sheep and *T. brucei*, though it should be noted that, in two other species, a tyrosine replaces the arginine 32, (33s), which interacts with the 2'-phosphate. The most important changes in sequence between the sheep and *T. brucei* enzymes, which may affect binding are Ala 11s to Gly 10, Lys75s to Gln 77 and Phe 83s to Thr 85.

The Cβ of Ala 11s in sheep 6PGDH protrudes into the bis-phosphate binding site. This residue corresponds to the central glycine of the generic fingerprint; the very small number of direct interactions of the bis-phosphate to the protein is almost certainly a consequence of this alanine. The substitution of glycine for alanine in the *T. brucei* enzyme should allow direct interactions between the enzyme and the $NADP^+$ bis-phosphate and has a further consequence in that the highly conserved valine 11 (Val 12s) faces towards the putative nicotinamide site in *T. brucei* 6PGDH and away from it in the sheep enzyme. Val 11 would provide further Van der Waals contacts for the nicotinamide ring. The substitution of Gly 10 in the *T. brucei* enzyme would suggest a tighter binding of coenzyme as reflected in the higher affinity.

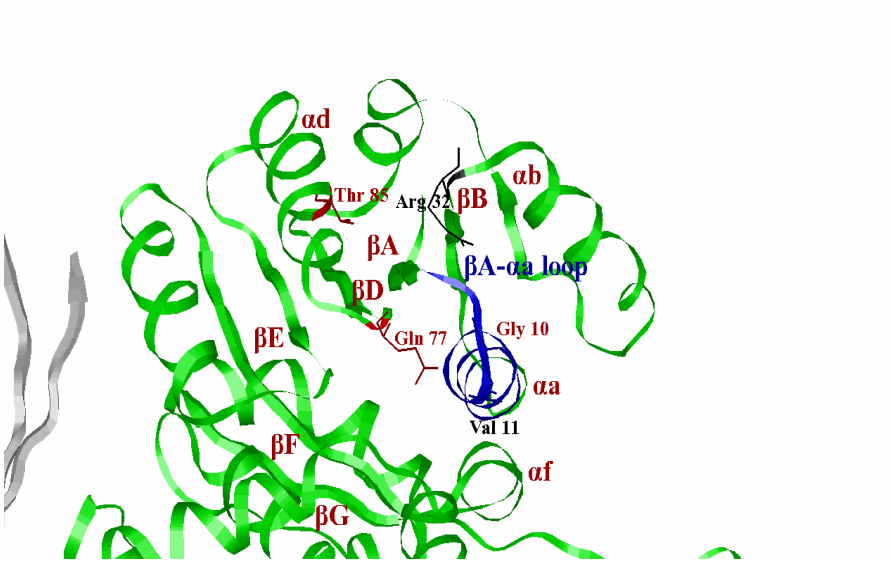

Fig. 8. Coenzyme binding site.

Functional asymmetry

6PGDH is a homodimer, but, in many species, it shows functional asymmetry [29-35]. For instance, both the yeast and sheep liver enzyme bind covalently two molecules of periodate-oxidized NADP, but, in the presence of 6PG, a half-site reactivity is acquired with only one subunit binding the NADP analogue, with the other subunit unable to bind even the adenylic moiety of the coenzyme [29,30]. These experiments suggest that when one subunit is involved in the ternary complex enzyme-6PG-NADP, the other subunit is unable to bind NADP and is thus inactive (Fig. 9). Also 6PGDH from human erythrocytes shows a half-of-the-sites reactivity, indeed it is able to bind two molecules of NADP, but only one of NADPH, suggesting that the binding of NADPH to one subunit affects the conformation of the other NADPH binding site; the free enzyme is unable to bind NADP and NADPH at the same time [32].

Moreover, negative cooperativity for NADP has been found in human erythrocyte [32] and rat liver [33] 6PGDHs, and stopped-flow experiments with the sheep

enzyme have indicated in the first turnover the formation of only one NADPH molecule per enzyme dimer [31]. The substrate binding site is made up of residues from both subunits, allowing the communication between the two active sites, which has also been shown by the decarboxylation activation of 6-phospho-3-keto-2-deoxygluconate by 6PG [34].

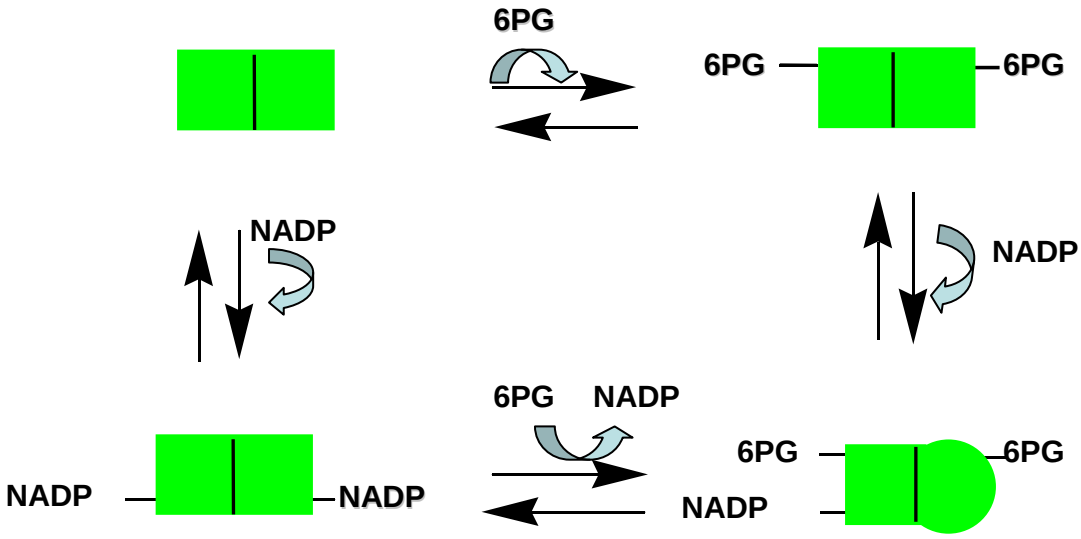

Fig. 9. Half of the site mechanism

Half-of-the-sites reactivity and conformational changes

All data presented so far point to half-of-the-sites reactivity and to conformational changes induced by 6PG. The half-of-the-sites reactivity requires that a change of one parameter of one subunit is communicated to the other subunit. The crystallographic studies have indicated that each active site of the enzyme contains amino acid residues from the coenzyme and the helix domains of one subunit and the carboxy

terminal tail of the other. Thus 6PG, binding to one active site, comes in contact with residues of all three domains of the two subunits; this binding may cause a shift of one subunit with respect to the other, possibly causing a conformational change not only in this active site but also in the other and in the dimeric interface [37]. However crystallographic data do not show any significant conformational change upon binding of substrate or coenzyme.

Instead, in solution, the binding of 6PG, phosphate or sulphate causes conformational changes in the enzyme molecule. Indeed, in their presence, the activity of yeast 6PGDH is much more stable against inactivation by seven proteolytic enzymes, acid, heat, cystamine, DTNB, urea, SDS [38], and different inactivating chemical reagents [39,40-44]. In presence of phosphate buffer the order of binding of 6PG and NADP to the enzyme is different than in triethanolamine buffer [31] and the reactivity of several thiol groups with DTNB reduced [45]. 6PG increases the reactivity with periodate-oxidized NADP [45,29]. All these data indicate that the binding of these compounds modifies in part the conformation of the enzyme in solution, making it, perhaps, more rigid.

All the crystallographic data were obtained with crystals prepared in ammonium sulphate. In the crystals each enzyme subunit has firmly bound three sulphate ions[15]; each of these ions bridges different segments of the protein chain in the same or in a different subunit stabilizing the conformation of the enzyme. Two of these sulphates bind to the active site and one is displaced by 6PG. The finding that the enzyme in the crystals does not show conformational change in presence of 6PG could be due to the fact that these changes were already induced by bound sulphate ions.

A hypothesis of alternating-site mechanism

It has been advanced [34] the hypothesis that the two enzyme subunits have an alternating role in the oxidative decarboxylation: while one of the two equal subunits catalyses the redox reaction, the other subunit, with a different conformation, catalyses the decarboxylation and tautomerization reactions. Then the two subunits alternate their conformation and role. On the basis of now available data, the molecule of the dimeric anzyme has the following properties:

1. presents a half-of-the-sites reactivity,
2. in one turnover produces only one NADPH molecule,
3. is able to bind simultaneously, but in different subunits, the substrate and its oxidation product,
4. when one subunit binds 6PG, the other is able to decarboxylate the intermediate,
5. when one active site binds 6PG and NADP, the other is unable to bind the coenzyme,
6. NADPH activates the reactions of decarboxylation and tautomerization, but the activation does not depend on its redox role.

In Fig. 10 a detailed hypothesis on the mechanism of action of 6PGDH is presented. For the sake of simplicity “INT” is the intermediate of the oxidative decarboxylation and “Ru5P” indicates both the ketonic and enolic forms of Ru5P. Likely, in this Figure ”decarboxylation” collectively indicates the tautomerization reaction and the release of carbon dioxide.

According this hypothesis, 6PG binds to one (B) of the two structurally equal subunits, inducing in both a different conformational change (step 1). Also NADP binds to the same subunit. Subunit B catalyzes (step 2) the redox reaction producing the intermediate and NADPH. Now 6PG binds to subunit A (step 3) inducing in both subunits a conformational change which promotes subunit B to catalyze the decarboxylation of the intermediate. The binding of NADP to subunit A induces the

release of the oxidative decarboxylation products from subunit B (step 4). Now in subunit A the redox reaction occurs (step 5) with the production of NADPH and the intermediate. Step 6 and 7 are a repetition of step 3 and 4, but the subunits exchange their role.

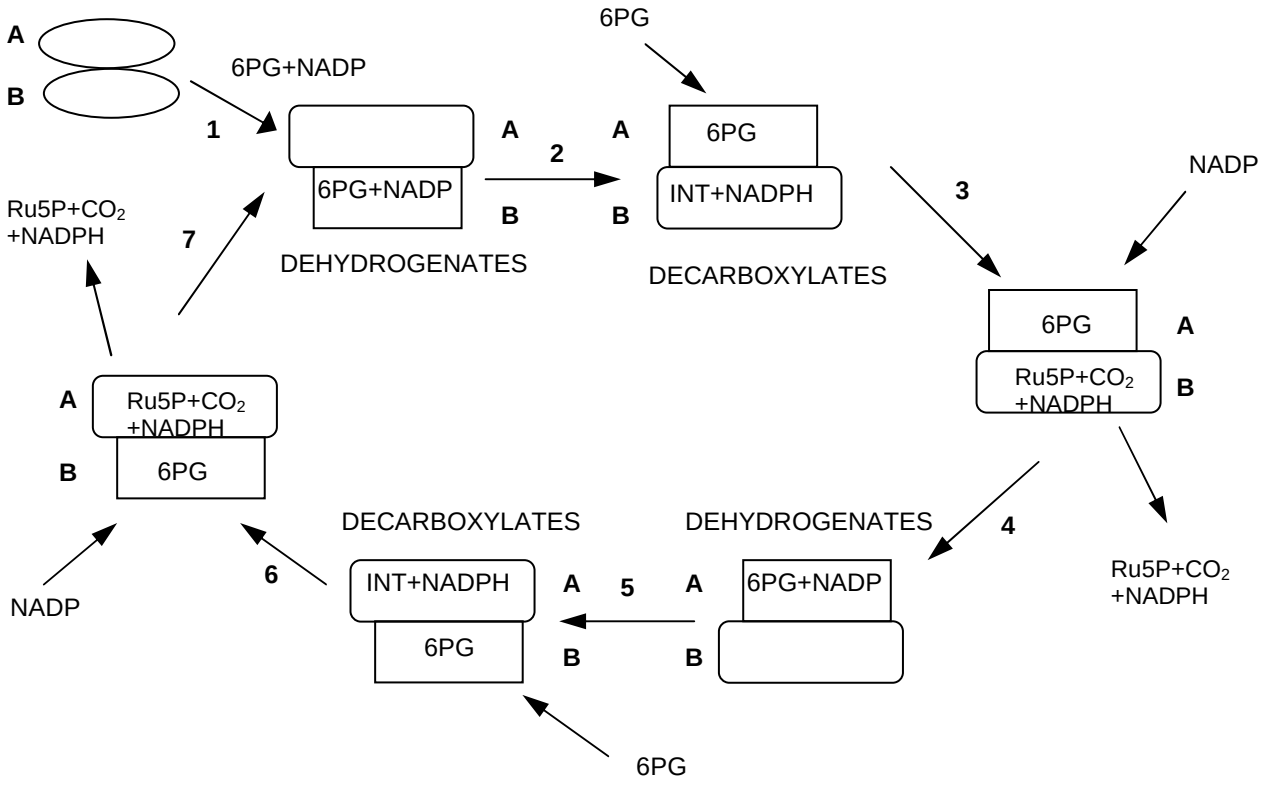

Fig. 10 Hypothesis of half-site mechanism

Inhibitors of *T. brucei* 6PGDH

Two reviews have dealt with *T. brucei* 6PGDH inhibitors as lead compounds for new drugs against African trypanosomes [46,47]. Since then, new better inhibitors have been found, which mimic the transition-state and high-energy intermediates of the enzymatic reaction of 6PGDH [48]. Hydrophobic analogues of these also revealed some anti-parasite activity [54]. A number of phosphorylated carboxylic acids derived from aldose sugars were tested against 6PGDH, two particularly notable inhibitors were identified. Both 4-phospho-D-erythronate (4PE) and 5-phospho-D-

ribonate (5PR) (Fig. 11, compounds **1** and **2**) were competitive with respect to substrate, with K_i values for the *T. brucei* 6PGDH equal to 130 and 950 nM respectively. Their selectivities for the *T. brucei* 6PGDH over the sheep liver one (ratio K_i sheep/ K_i *T. brucei*) were measured at 83-fold and 70-fold respectively. K_i values for both are under the K_m for 6PG (= 3.5 μM), indicating that they mimic high-energy reaction intermediates (Fig. 2) rather than the substrate *per se* [46,49].

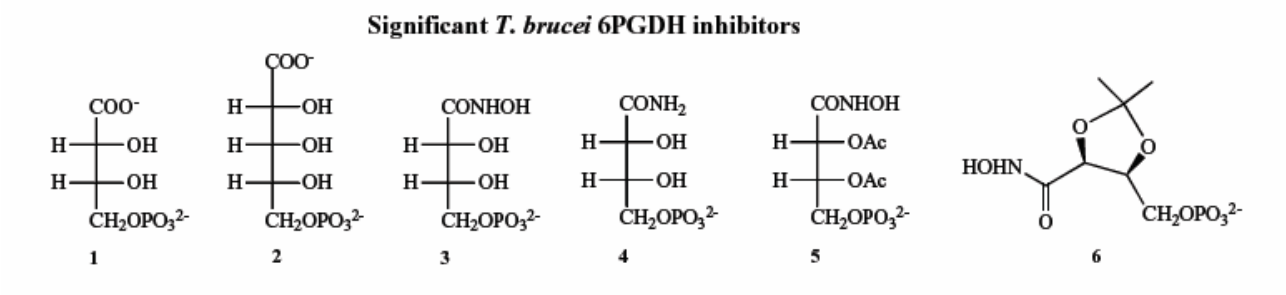

Fig. 11. Structures of some substrate analogues (Ac=Acetyl group).

Another potent and selective *T. brucei* 6PGDH inhibitor is 4-phospho-D-erythronohydroxamate (Fig. 11, compound **3**), synthesized specifically to mimic the high-energy intermediates produced following the second (decarboxylation) step of the catalyzed reaction, shown in Figure 2. This hydroxamate, with a K_i = 10 nM and selectivity of 254-fold for the parasite enzyme over the sheep liver enzyme, is the compound with the highest affinity for the *T. brucei* 6PGDH reported to date and it also shows the highest selectivity for the parasite over the sheep liver enzyme [48].

In Table 1**,** inhibition constants versus 6PG (K_i) at pH 7.5 (which is the enzyme optimum pH) for all *T. brucei* 6PGDH inhibitors, which are shown in the figures included in this text, are reported, together with selectivity values over the sheep liver enzyme (ratio sheep liver 6PGDH K_i / *T. brucei* 6PGDH K_i).

Compound	K_i versus substrate (μM)	Selectivity (K_i sheep/ K_i *T.brucei*)
1	0.13	83
2	0.95	70
3	0.01	254
4	1.52	25.7
5	0.08	4.5
6	0.035	31.4

Table 1. 6PGDH inhibition constants of compounds in fig. 11.

To better understand why these analogues have high affinity and to help in rational drug design, we undertook a thermodynamic characterization of substrate and analogue binding to *T. brucei* 6PGDH, in both binary and ternary complexes, with NADP, the coenzyme analogue 3-amino-pyridine adenine dinucleotide phosphate (aPyADP) (Fig.18) or NADPH. We show that the ternary complexes with the oxidized coenzyme and with aPyADP display half-site reactivity, and that 4PE, but not 5PR, is a transition state analogue (Fig. 12).

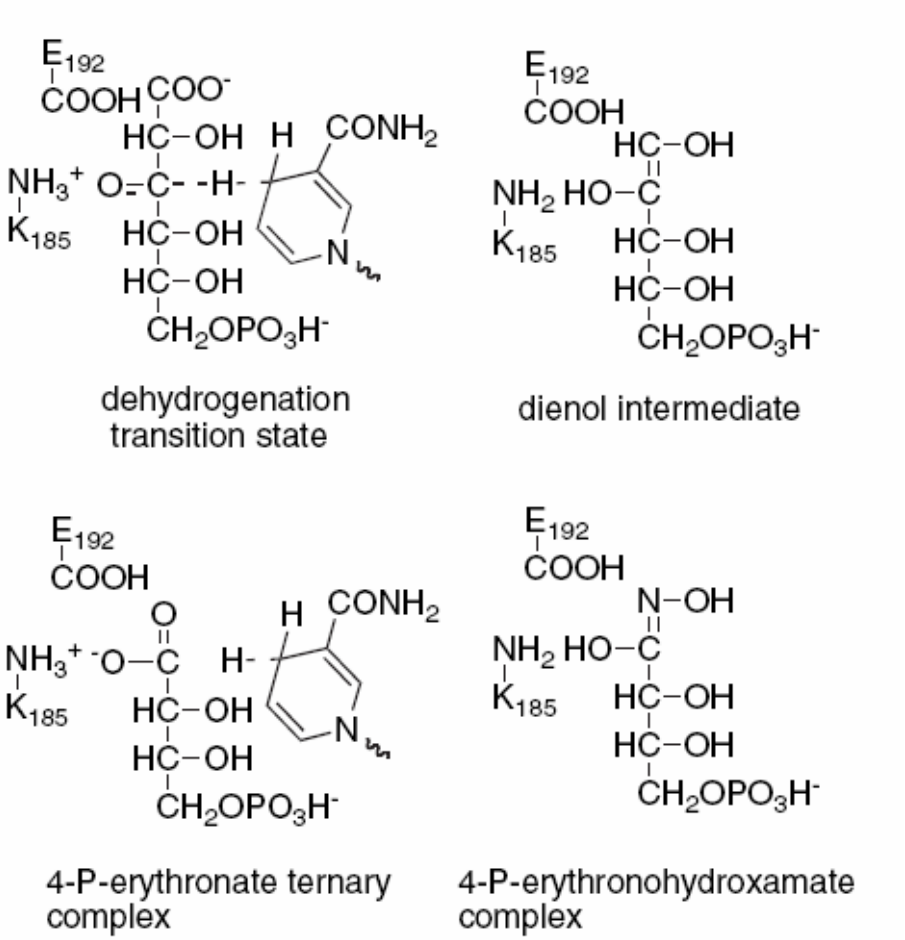

Fig.12. Protonation states of the two main active site amino acid residues in different reaction steps and in the complexes with 4PE or 4PEX.

The reverse reaction

Despite the catalytic mechanism of 6PGDH has been widely investigated, very little is known on the last steps of the reaction, and in particular on the conversion of the dienol to Ru5P. In the oxidative decarboxylation this step follows the irreversible release of CO_2, so its weight on the overall kinetics is shielded. The enzyme follows a rapid equilibrium bi-ter sequential mechanism, with random order of substrate addition both in the direct reaction, the oxidative decarboxylation, and in the reverse reaction, the reductive carboxylation [75]. The enzyme dependent stereospecific keto-enol conversion of Ru5P occurs even in the absence of CO_2 [14], and it has been

shown that this reaction has the absolute requirement of NADPH, that does not have a redox role and can be substituted by non-reducing analogues [73]. The only information about the carboxylation reaction is that CO_2 is the true substrate, but the presence of a CO_2 binding site has not been clearly demonstrated.

^{2}H and ^{13}C isotope effects have shown the both dehydrogenation and decarboxylation steps are partially rate limiting, while solvent isotope effect evidenced a kinetically significant isomerization step preceding the dehydrogenation. A study of the kinetic isotope effects in the reverse reaction, the reductive carboxylation, could give the additional information required for a better comprehension of the “hided” steps, and a complete description of the energy profile of the reaction.

AIM OF THE THESIS

6-Phosphogluconate dehydrogenase is a validated drug target in African trypanosomes [46]. A number of compounds have been discovered which show selective and potent inhibition of the parasite enzyme [53]. The structure of the enzyme from both the trypanosome and mammalian source is known; there do not appear to be significant structural differences between the enzymes, although it has been possible to discover very selective inhibitors of the trypanosome enzyme [24]. Unfortunately the inhibitors discovered do not have activity against trypanosomes, which is probably due to their highly charged and polar nature [53]. Nevertheless some recently developed parent compounds with phosphate masking groups, which are able to deliver active compounds into parasites, show a good level of trypanotoxicity [54]. One objective of this work is to better understand the inhibition mechanism of some substrate analogues in the 6PGDH of T. *brucei* through thermodynamic characterization.

Another objective is to investigate the action mechanism of 6PGDH and this has been done by two different approaches. Firstly we have prepared the mutants of Glu192 and Lys 185, the residues that are postulated to assist the catalytic steps, and we have investigated the thermodynamics of substrate binding to the enzyme through isothermal titration calorimetry (ITC). The comparison of ITC data of the *wild type* with the mutant enzymes is helping us to understand the role of these residues in the change induced in the enzyme by the substrate binding. Moreover since the lysine residue is thought to be protonated in the free enzyme and non protonated in the enzyme-substrate complex, this raises the question whether the binding of the substrate causes a proton release in the medium or an intramolecular proton transfer occurs. To better understand the protonation state of the enzyme-substrate complex, we have studied by ITC the release-uptake of hydrogen ions during the formation of the enzyme-6PG complex in the 6PGDH from T. *brucei* by comparing the *wt* enzyme with several mutants of the enzyme.

A second approach was the study of the reverse reaction of the 6PGDH by kinetic isotope effects. This approach, together with the data already present in literature, allows the construction of the energy profile of the whole reaction.

MATERIALS AND METHODS

Preparation of wild type 6-Phosphogluconate Dehydrogenase of *T. brucei*.

Overexpression of the *T. brucei* enzyme in *E. coli*.

Plasmid pT7gnd was transformed into *E.coli* strain BL21 (DE3). pT7gnd is derived from cloning of the gene gnd into the vector pET3a, with the ATG initiation codon oriented adjacent to the bacteriophage T7 RNA polymerase promoter. BL21 (DE3) are *E. coli* cells with the phage DE3 encoding T7 RNA polymerase under the control of the lacUV5 promoter. A single transformed colony was grown overnight at 37°C in LB/amp (Luria Bertani broth plus ampicillin). The next morning the overnight culture (30 ml) was added to 0.8 liters of LB/amp and grown with agitation in a 2-liter conical flask at 28°C until the culture reached an optical density of 0.6 at 600nm. At this point the lac operon inducer isopropylthiogalactopyranoside (IPTG) was added to a final concentration of 0.4 mM. The culture was left incubating at 28 °C for 4 h, after which the cells were harvested by centrifugation at 4000 rpm for 10 minutes.

Purification of plasmid DNA

Plasmid DNA purification was performed by using a Miniprep Kit (Quiagen). This method consists of three basic steps: alkaline lysis of bacterial cells, selective absorption of plasmid DNA on a silica membrane and washing and elution of plasmid in low ionic strength buffer. It is an easy and fast method that allows to get pure DNA for cloning and for sequencing.

Determination of DNA concentration

The Determination of DNA concentration is done both by ultraviolet spectrometry (UV) and valuation after agarose gel electrophoresis.

Spectrophotometric determination

The DNA concentration was assayed both at 260 nm and 280nm:

DNA Concentration (μg/ml) = A_{280nm} x 50 μg/ml

The ratio OD_{260}/OD_{280} must be ≥ 1.7 for pure preparation of DNA, if the ratio is < 1.7 it means that in the sample there is protein contamination.

Electrophoresis in agarose gel

The agarose gel was prepared in buffer TAE (0,04 M Tris, 1mM EDTA 5 mM sodium acetate, taken to pH 7.5 with glacial CH_3COOH) adding ethidium bromide 0,4 μg/ml. Before loading, 0.2 volumes of the following buffer: 0.25 % (p/v) bromine phenol dye, 100 mM EDTA, 50% (v/v) glycerol is added to the sample. After the electrophoretic run, DNA is seen by UVtransillumination, for the fluorescence effect of the ethidium bromide that binds to double stranded DNA.

+

Site- Directed Mutagenesis

The QuickChange II site-directed mutanegesis Kit (Stratagene) was used to introduce nucleotide changes according to manufacturers' specifications directly into the *T. brucei* 6PGDH gene, cloned into the expression vector pET3a.

The plasmids extraction was from bacterial stock JM109 (Genotype: F' [*tra*D36, *pro*AB^{+}, *lac*I^{q}, *lac*ZΔ(M15)], *rec*A1 *edn*A1 *gyr*A96 *thi hsd*R17 *sup*E44 *rel*A1 Δ(*lac-pro*AB). The stock JM109 has been used for cloning of the gene of the wild type enzyme. The QuikChange II site-directed mutagenesis method is performed using PfuUltra™ high-fidelity (HF) DNA polymerase for mutagenic primer-directed replication of both plasmid strands with the highest fidelity. The basic procedure utilizes a supercoiled double-stranded DNA (dsDNA) vector with an insert of interest and two synthetic oligonucleotide primers, both containing the desired mutation (see Figure 13). The oligonucleotide primers, each complementary to opposite strands of the vector, are extended during temperature cycling by PfuUltra HF DNA polymerase, without primer displacement. Extension of the oligonucleotide primers generates a mutated plasmid containing staggered nicks. Following temperature cycling, the product is treated with Dpn I. The Dpn I endonuclease (target sequence: 5´-Gm6ATC-3´) is specific for methylated and hemimethylated DNA and is used to digest the parental DNA template and to select for mutation-containing synthesized DNA. (DNA isolated from almost all *E. coli* strains is dam methylated and therefore susceptible to Dpn I digestion.) The nicked vector DNA containing the desired mutations is then transformed into XL1-Blue supercompetent cells.

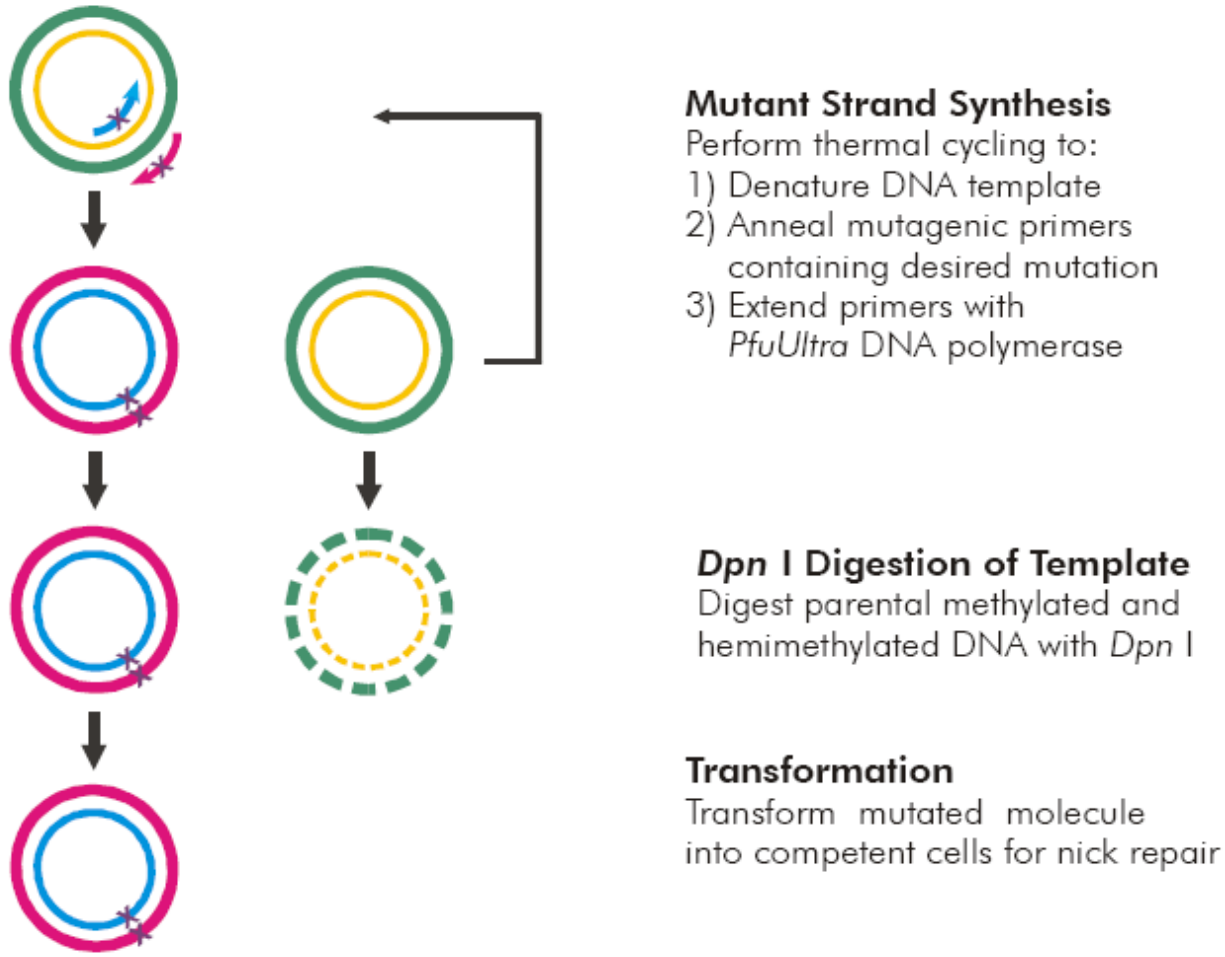

Fig. 13. Overview of the QuickChange II site-directed mutagenesis method.

In table 2 the sequence of one of the two oligonucleotides for every mutation is reported.

K185H	5'-GGATCATGCGTG**CAT**ATGTACCACAATTCG-3'
K185R	5'-GGATCATGCGTG**CGT**ATGTACCACAATTCG-3'
E192Q	5'-GATGTACCACAATTCGGGT**CAA**TACGCCATTTTGCAAATCTG-3'
H188L	5'-GGCGTATTCACCCGAATT**AAG**GTACATCTTCACGCATGATCCC-3'
C372S	5'-GCCCTGCAAAAT**GCT**ACCGGCGCGGA-3'

Table 2 Primer oligonucleotides synthetized by of MWG-biotech AG.

The reaction protocol is:

reaction buffer (10X) 5µl

dsDNA template (5 -50 ng) 2 µl

Forword Oligonucleotide (125 ng) 12.5 µl

Reverse Oligonucleotide (125 ng) 12.5 µl

dNTP mix 1 µl

ddH_2O to a final volume of a 50 µl

Then add

1 µl di *PfuTurbo* DNA polymerase (2.5 U/µl) and let things go the reaction in the following way:

Segment	Cycles	Temperature	Time
1	1	95 C°	30 seconds
2	12-18	95 C° 55C° 68C°	30 seconds 1 minute 1 minute/kb of plasmid length

Following temperature cycling, place the reaction on ice for 2 minutes to cool the reaction to ≤ 37°C.

Add 1 µl of *Dpn* I restriction enzyme (10U/ µl), and gently mix reaction by pipetting the solution. Spin down the reaction mixtures in a microcentrifuge for 1 minute and immediately incubate reaction at 37°C for 2 hours to digest the parental supercoiled dsDNA.

Transformation into XL1- Blue Supercompetent Cells

Gently thaw the XL1- Blue supercompetent cells on ice. For each sample reaction to be transformed, aliquot 50 µl of the supercompetent cells in a tube.

Transfer 1 µl of the *Dpn* I- treated DNA from each sample. Swirl the transformation reactions gently to mix and incubate the reactions on ice for 30 minutes.

Heat pulse the transformation reactions for 45 seconds at 42°C and then place the reactions on ice for 2 minutes.

Add 0.5 ml of NZY+ broth (10g of NZ amine, 5g of yeast extract, 5g of NaCl 12.5 ml of 1 $MgCl_2$, 12.5 ml of 1 M $MgSO_4$ and 20ml of 20% (w/v) glucose per liter adjust pH 7.5) preheated to 42°C and incubate the transformation reactions at 37°C for 1 hour with shaking at 225-250 rpm.

Plate 250 µl of each transformation reaction on agar plates containing the appropriate antibiotic for plasmid vector.

Incubate the transformation plate at 37 °C for > 16 hours.

Transformation into *E. coli* strain BL21 (DE3)

The following steps are the extraction of plasmidic DNA from a single colony and sequencing of the entire coding region of mutants *T. brucei* 6PGDH to check that only the single mutation is present, using the dideoxynucleotide chain-termination method. Once mutated sequence is obtained, it is introduced into *E. coli* strain DL21 (DE3) for inducible expression.

Enzyme purification

The recombinant *T. brucei* 6PGDH, overexpressed in *Escherichia coli*, was purified according to a technique that was slightly modified compared to the original of Barrett [49,50].

Cells were harvested by centrifugation (4,000 rpm, 10min), resuspended in 15ml of cell lysis buffer (50 mM TEA, 0.1 mM EDTA and 1mM βmercaptoethanol pH 7.5) and sonicated.

Cell debris and insoluble material were then spun down (40,000rpm, 30min). The supernatant was applied to a 15 ml DEAE-Sepharose column equilibrated with TEA buffer, which was then washed with the same buffer and the flow through material absorbing at 280 nm was loaded directy onto a 5 ml 2',5'-ADP-Sepharose column, equilibrated with TEA buffer diluted 50 x.

After washing, the enzyme was eluted with $Na_4P_2O_7$ 150 mM containing 1mM EDTA pH 7.2 and the specific activity assayed in buffer containing 0,6mM 6PG and 0.26 mM $NADP^+$.

The whole purification lasted less than one day and was monitored both by SDS-PAGE and activity assays. Enzyme was stored in the presence of 50% glycerol at -20°C.

Enzyme activity

One unit of enzyme activity is the amount of enzyme that produce one μmol of NADPH in one minute. The absorptivity molar to 340 nm of NADPH is 6,220. The specific activity of the enzyme has been calculated as the number of UI divided by the number of mg of protein.

Determination of protein concentration

Protein content was determined with the spectrophotometer at 280 nm, assuming that a solution containing 1mg/ml of protein have an absorbance of 1 O.D. A solution containing 1 mg/ml of pure 6PGDH has at 280 nm an absorbance of 1.023. Since a single subunit of 6PGDH has a molecular weight of 52 kDa, in 1mg of protein there are 19.2 nmol of subunit.

Assay of activity for 6PGDH dehydrogenase

The assay is based on kinetic measurement of NADPH that has a maximum absorption at 340 nm. The reaction mixture contains 0.6 mM 6PG and 0.26 mM NADP in 50mM TEA buffer pH 7.5 with EDTA 0,1mM. The initial velocity is measured adding 15 µg of 6PGDH enzyme to 1 ml of reaction mixture, which is followed spectrophotometrically, at 340 nm, for the reduction of NADP.

Electrophoresis in polyacrylamide gel (SDS PAGE)

4 µg/ µl of enzyme are denatured at 100°C for 5 minutes in the presence of the reducing agent 2-Mercaptoethanol and loaded onto a gel of polyacrylamide. The migration has been made into electrophoresis buffer during 45 minute with an amperage of 25 mA. The proteins were coloured with a solution of Comassie blue (3% p/v Comassie Brillant Blue, 40% v/v acetic acid, 40% v/v methyl alcohol, in water) at room temperature.
Destaining is done in 7% v/v acetic acid, 7% v/v isopropyl alcohol, 1% methyl alcohol.

Preparation of inhibitors

Ribose-5-phosphate and erythrose-4- phosphate were purchased. 5PR and 4PE were prepared by bromide oxidation [51] of ribose-5-phosphate and erythose-4-phosphate, respectively. The concentration of 5PR and 4PE were determined by measuring the concentration of organic phosphate [52].

Determination of the kinetic parameters and pH studies

All assays were performed, in the direction of oxidative decarboxylation of 6 phosphogluconate, measuring the initial rate, when no deviation from linearity was observed (the minimum time for linearity was 1 min with the lowest concentration of NADP). Measurements were performed at 20°C either spectrophotometrically measuring at 340 nm the production of NADPH in a Kontron Uvikon 930 spectrophotometer. Concentrations of $NADP^+$ and 6-phosphogluconate were determined enzymatically.

Rates obtained were always strictly proportional to the amount of enzyme added.

Kinetics parameters were determined from Lineweaver-Burk plots. For determination of K_m for 6PG, NADP was at a concentration of 0.2mM, while concentrations of 6PG were varied between 6 and 50 μM. For determination of K_m for NADP, the 6PG were at a concentration of 0.5mM, while concentrations of NADP were varied between 5 and 40 μM. The buffers for the different pH ranges were used in combination at 10mM each: TEA/HCl pH 7.5-8.4, Hepes/NaOH pH 6.8-8.2, MES/NaOH pH 5.5-6.7.

Reactivity of cysteines

The method (G. Ellman reaction) is based on the capacity of sulphidrilic groups of cysteines to react with 5,5- ditiobis-2-nitro benzoic acid (DTNB), developing a spectrophotometrically measurable complex.
The reactivity of cysteines in the reaction has been measured in TEA buffer pH 7.5 at 20 °C, using a molar ε at 412 nm of 13600 for residue. The enzymes were used at a concentration of 4 μM.

Isothermal titration calorimetry

Isothermal titration calorimetry (ITC) is suitable for characterizing both low affinity interactions (e.g. protein network regulation and natural ligands) and high affinity interactions (e.g. rational drug design). Considering the advanced technological level reached as well as the outstanding quality of the information accessible through this technique, ITC is expected to play a very prominent role in the next years in the areas of rational drug design and protein network regulation.
Calorimetry measures directly the heat associated with a given process, which, at constant pressure, is equal to the enthalpy change in that process, ΔH. Due to sensitivity and accuracy reasons, the calorimeters used to characterize binding processes belong to the category of titration calorimeters with dynamic power compensation operating at constant temperature (isothermal titration calorimetry). A detailed description of the instrument and of the technique can be found in the literature [56-64]. Briefly, the macromolecule solution is located inside the sample cell and ligand solution in the injector syringe. A feedback control system supplies thermal power continuously to maintain the same temperature in both reference and sample cells. Any event taking place in the sample cell, usually accompanied by heat, will change the temperature in that cell and the feedback control system will

modulate the power supplied in order to minimize such temperature imbalance. A sequence of injections is programmed and the ligand solution is injected periodically into the sample cell (Fig. 14).

Integration of the calorimetric signal and nonlinear least-squares analysis of the resulting binding data were performed to determine the equilibrium association constant, K_a, the binding enthalpy, ΔH, and the stoichiometry of the interaction, n. The Gibbs free energy of binding, ΔG, and the entropic contribution to the binding free energy, ΔS, were calculated from the resolved parameters using the relationships:

$$\Delta G = - RT \ln K_a$$

$$\Delta G = \Delta H - T \Delta S$$

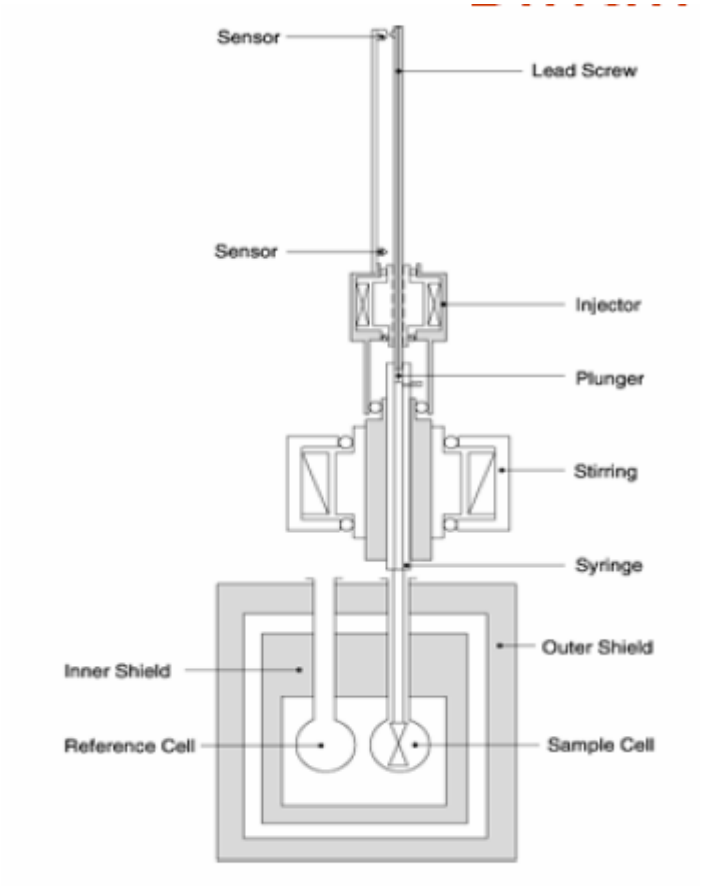

Fig. 14. Scheme of microcalorimeter ITC.

ITC measurements

Before each experiment, the enzyme was dialysed exhaustively and the titrant was diluted in dialysis buffer. All solutions were properly degassed before the titration experiments. The enzyme (4-6 μM dimer) was placed in the stirred cell and titrated with a total of 23 injections of 10 μL of ligand, at 380 s intervals. An initial preinjection of 5 μL volume was made, and the result from this injection was not used for data analysis. Heats of dilution and mixing, obtained by blank titrations, without the enzyme, were subtracted from the heats obtained with enzyme titrations. For ternary complex studies, the first ligand was added at the same concentration in both enzyme and titrant to keep the concentration constant during the experiment.

The enzymatic activity was measured before and after each experiment to verify whether enzyme inactivation occurred during titration.

Experiments were performed in 50 mm buffer, with 0.1 mM EDTA and 1 mM 2-mercaptoethanol. At pH 7.5 three buffers were used: Hepes (ΔH_{ion} = 5.03 kcal mol^{-1}), triethanolamine (ΔH_{ion} = 7.932 kcal mol^{-1}) and Tris (ΔH_{ion} = 11.3 kcal mol^{-1}). At different pH other buffers were also used: Cacodylate (ΔH_{ion} = 0.7 kcal mol^{-1}) and MOPS (ΔH_{ion} = 5.22 kcal mol^{-1}).

The buffer-independent binding enthalpy ΔH_0 and the number of hydrogen ions exchanged were calculated by the least-squares fitting of the experimental enthalpy in different buffers:

$$\Delta H_{obs} = \Delta H_0 + nH^+ \Delta H_{ion}$$

$$nH^+ = \frac{\Delta H^1{}_{obs} - \Delta H^2{}_{obs}}{\Delta H^1{}_{obs} - \Delta H^2{}_{obs}}$$

where ΔH_{obs} is binding enthalpy experimentally observed, while ΔH_{ion} is the buffer ionization enthalpy.

Measurements were performed at 20 °C in a VP-ITC microcalorimeter (Microcal, Northampton, MA, USA), and the data were fitted by nonlinear least-squares fitting using Origin™ software provided by the instrument manufacturer.

Fluorescence measurements

Titration of the 6PGDH-aPyADP complex with 6PG was performed fluorimetrically, with a Perkin-Elmer LS55 spectrofluorimeter at 20°C. By this method the decrease of fluorescence emission by the aPyADP at 410nm, on addition of 6PG was measured (excitation at 330nm).

1ml of solution containing 19 µM enzyme and 350 µM aPyADP was titrated with additions (1-2 µl each) of 5.54 mM 6PG.

The dissociation constants were estimated by using Scatchard plots in the form:

$$\frac{\Delta F}{[substrate]} = \frac{1}{K_d}(\Delta F_{max} - \Delta F)$$

where ΔF is the observed fluorescence decrease, and ΔF_{max} the decrease at infinite substrate concentration.

Isotope effects

6PGDH from *Candida Utilis* was purified as already described [71]. The specific activity of the purified enzyme was 46 µmoles $min^{-1}mg^{-1}$. Stereospecifically labeled (*1h*), (*1d*) and (*1t*) 1Ru5P were prepared enzymatically from 6PG [14]. 1(*1t*)Ru5P

was prepared as previously described [14], and the specific activity of purified Ru5P was 58 cpm/nmole. For the preparation of 1(*1d*)Ru5P, buffer was prepared in 99.9% D_2O, liophylized two times to remove exchangeable hydrogen, and redissolved in D_2O. The pH (pD) was calculated from pHmeter reading + 0.3. The enzymes used in the preparation were previously precipitated by 70% saturated ammonium sulfate, washed two times with 70% saturated ammonium sulfate in D_2O, and finally dissolved in the buffer. The isotopic substitution was estimated by NMR and was found 94%. Ru5P was purified from the reaction mixture by ion exchange chromatography and used within two days. When the Ru5P was stored for longer times, it was rechromatographed before the experiments. The concentration of Ru5P was determined colorimetrically [72]. 1,6-NADPH was prepared by $NaBH_4$ reduction of $NADP^+$ and purified by DEAE Sepharose chromatography as already reported [73].

Isotope exchange measurement

Tritium release from 1(*1t)*Ru5P was measured as previously reported [73]. For the measurements of tritium uptake, (*1h*)Ru5P and (*1d*)Ru5P were dissolved at the desired concentrations in Tris-acetate buffer, containing tritiated water (specific radioactivity 9.7 cpm/nanom). Contaminating CO_2 was removed from the buffer by purging the solution with helium. Enzyme (0.062 mg) and NADPH (0.1 mM) were added, and the reaction was allowed to proceed at 24 °C for 30 min. The samples were then frozen, lyophilized, redissolved in water and loaded on a small Dowex1 column. The resin was washed extensively with water, to remove any unbound radioactivity, and Ru5P was eluted with 4 x 0.5 ml of NaCl O.5 M. The eluate was assayed for radioactivity and Ru5P.

Reverse reaction measurements

The effect of isotope substitution on Ru5P in the reverse reaction was measured by comparing the relative reaction rates of the (*1h*) and (*1d*) Ru5P. The reaction was carried out in O.1 M $NaHCO_3$ saturated with CO_2, pH 6.9, 0.1 mM NADPH, 1.24 µg of 6PGDH, measuring the decrease of the absorbance of NADPH. Tritium isotope effect was measured in the same $NaHCO_3/CO_2$ buffer, pH 6.9, with 1mM NADPH, 0.062 mg of 6PGDH, 5.0 mM isocitrate and 5 units of isocitrate dehydrogenase. At the desired times 0.1 ml samples were withdrawn from the reaction mixture and loaded on a small Dowex1 column. The column was washed extensively and Ru5P was eluted with 0.5 M NaCl, assayed and counted as described above.

Data treatment

Data were fitted with equation 1 and 2 for 1(*1h*)Ru5P and 1(*1d*)Ru5P respectively.

$$v = VA/(K_A+A) \quad (1)$$

$$v = VA/((K_A(1+f_iE_{V/K})+A(1+f_iE_V)) \quad (2)$$

where v and V are the initial and maximal velocity, K_A is the Michaelis constant for the variable substrate, A is the concentration of the variable substrate, fi the fraction of deuterium label in the substrate, E_V and $E_{V/K}$ the isotope effects minus 1 on V and V/K [74, 75].

$^T(V/K)$ was calculated from equation 3 at 10, 20 and 30% of substrate conversion:

$$^T(V/K) = \log(1-f)/\log[(1-f)AS_t/AS_0] \quad (3)$$

where ASt and AS_0 are the specific radioactivity at time t and time 0 respectively, and *f* is the fraction of the substrate reacted.

The overall kinetic equation is

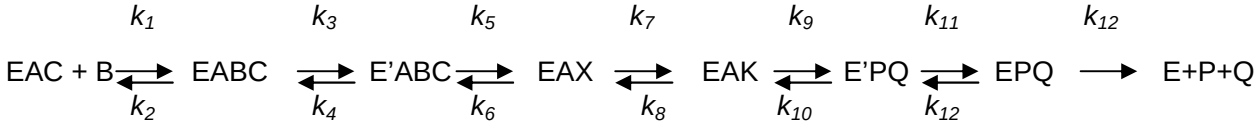

where A is NADPH, B Ru5P, C is CO_2, P and Q are 6PG and NADP respectively. X stays for the enol form of Ru5P and K for the 3K6PG. Accordingly to Northrop the isotope effects are

$$ {}^{D}(V/K) = \frac{{}^{D}k_5 + c_f + c_r\,{}^{D}K_{eq}}{1 + c_f + c_r} \tag{4} $$

$$ {}^{T}(V/K) = \frac{{}^{D}k_5^{1.441} + c_f + c_r\,{}^{D}K_{eq}^{1.441}}{1 + c_f + c_r} \tag{5} $$

$$ {}^{D}(V) = \frac{{}^{D}k_5 + c_{fV} + c_r\,{}^{D}K_{eq}}{1 + c_{fV} + c_r} \tag{6} $$

where

$$ c_f = k_5 / k_4 \tag{7} $$

$$ c_r = k_6 / k_7\left(1 + k_8 / k_9\left(1 + k_{10} / k_{11}\right)\right) \tag{8} $$

$$ c_{fV} = \frac{k_5 k_3}{k_3 + k_4}\left[1 + 1/k_7\left(1 + k_8/k_9\left(1 + k_{10}/k_{11}\right)\right) + 1/k_9\left(1 + k_{10}/k_{11}\right) + 1/k_{11}\right] \tag{9} $$

$^{D}K_{eq}$ was assumed to be 0,99 [77].

Intrinsic isotope effect was calculated from the equation:

$$ \frac{{}^{D}(V/K) - 1}{{}^{T}(V/K) - 1} = \frac{{}^{D}k_5 - 1 + c_r\left({}^{D}K_{eq} - 1\right)}{{}^{D}k_5^{1.441} - 1 + c_r\left({}^{D}K_{eq}^{1.441} - 1\right)} \tag{10} $$

PART I RESULTS AND DISCUSSION

Studies on the *wt* enzyme

Substrate and inhibitor binary complexes

The binding parameters for 6PG, 5PR and 4PE of *T. Brucei* 6PGDH wild type are reported in Table 3. The best fit of the average number of binding sites is slightly lower than two sites per dimer, reflecting the presence of some inactive enzyme.

Although the observed K_d values for 6PG and 5PR are very close to their K_m and K_i values, respectively, 4PE has a higher K_d value than the K_i value measured previously. The enthalpy change measured experimentally in titrations with 6PG arises primarily from the buffer protonation (Table 3); indeed, the release of 0.4 hydrogen ions was calculated from measurements in different buffers. The buffer-independent enthalpy change for the binding of 6PG is low and positive, 0.174 kcal mol^{-1}, and the binding is totally entropy driven.

The buffer-independent enthalpy change for the binding of 5PR and 4PE is negative (Table 3), with the release of only a small fraction of hydrogen ions (0.029 for 4PE and 0.018 for 5PR); however, for the substrate analogues also, the main contribution to binding comes from an increase in entropy.

In all cases, the binding is entropy driven, and desolvation of the phosphorylated sugars appears to give the major contribution to the binding entropy. It has been shown that the binding of inorganic phosphate to the complex between porcine elastase and the turkey ovomucoid third domain has favourable entropy and unfavourable enthalpy as a result of the release of strongly immobilized water molecules [70]. Phosphorylated sugars should show a similar behaviour, and the major part of the entropy gain observed could arise from the phosphate group.

Furthermore, we observed that TΔS decreases by about 500–700 cal by shortening the carbohydrate chain for each carbon atom (Fig.15), probably reflecting the water molecules immobilized by hydrogen bonds with the sugar hydroxyl. Thus, the high entropy gain obtained by the desolvation of the ligands can overcome the entropy loss caused by the immobilization of the carbohydrate chain.

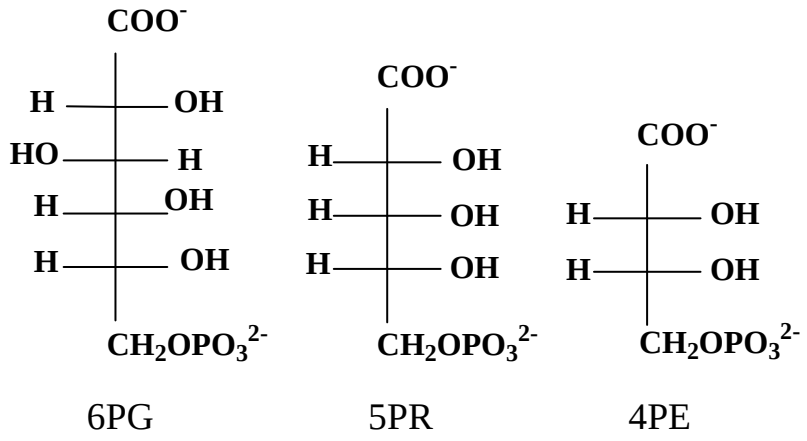

Fig.15. Structures of 6PG, 5PR and 4PE.

The enthalpy changes should also be discussed. The binding enthalpy for the inorganic phosphate to the elastase-ovomucoid third domain complex is about +3 kcal mol^{-1}. In this complex, there is only one ionic bond, whereas, in 6PGDH, the phosphate group of 6PG forms two ionic bonds with R289 (R287 in the sheep liver sequence, R289 in the *Lactococcus lactis* enzyme shown in fig. 16) and R453 (R446 in the sheep liver sequence, R447 in the *L. lactis* enzyme, fig.16).

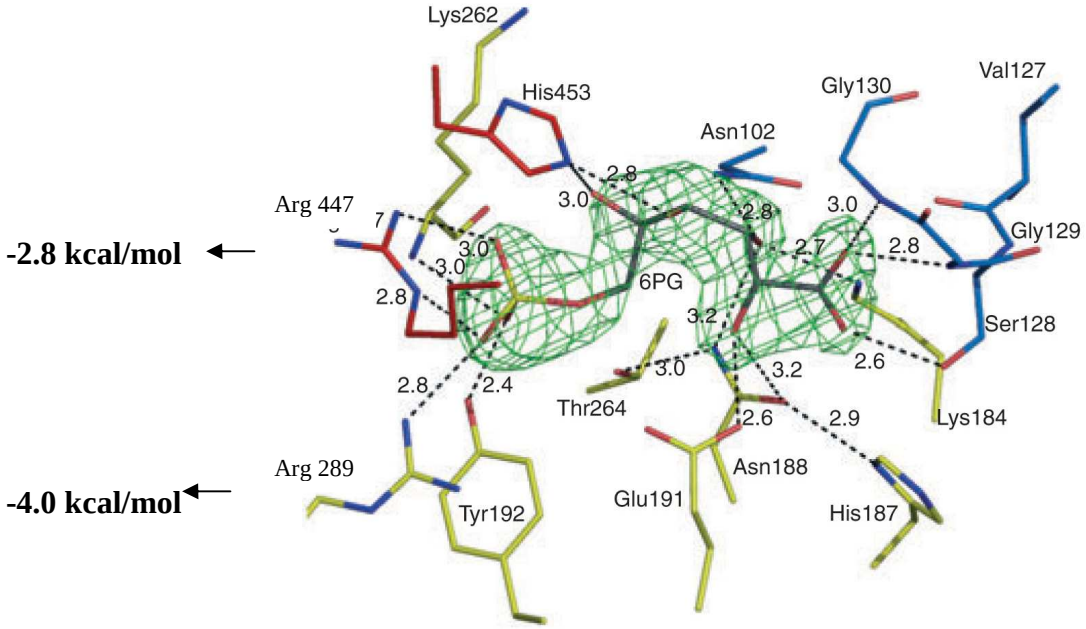

Fig.16. Structure of *L. lactis* enzyme at the substrate binding site.

It has been shown by site-directed mutagenesis of sheep liver 6PGDH that these two arginine residues can contribute to the binding free energy by -4.0 and -2.8 kcal* mol^{-1}, respectively. Thus, the additional enthalpy gain generated by a second ionic bond could overcome the positive enthalpy change generated by desolvation of the phosphate group.

Ligand	**K_d (μM)**	**K_mK_i (μM)**	**ΔH_0(cal mol^{-1})**	**$T\Delta S_0$(cal mol^{-1})**	***n*H$^+$**	**Sites/dimer**
6PG	4.96 ± 0.69	3.5	173.8	7398	-0.46	1.47 ± 0.06
5RP	1.35 ± 0.19	0.95	-1330	6626	-0.018	1.33 ± 0.1
4EP	2.86 ± 0.79	0.13	-2381	5111	-0.029	1.83 ± 0.3

Table 3 Binding parameters of substrate and substrate analogues to 6PGDH from *Trypanosoma brucei*, K_mK_i values are taken from [49,55].

Nevertheless, although the binding enthalpy of the inhibitors is negative, the binding enthalpy of 6PG is small and positive. This correlates with the proton release during binding (Fig.17).

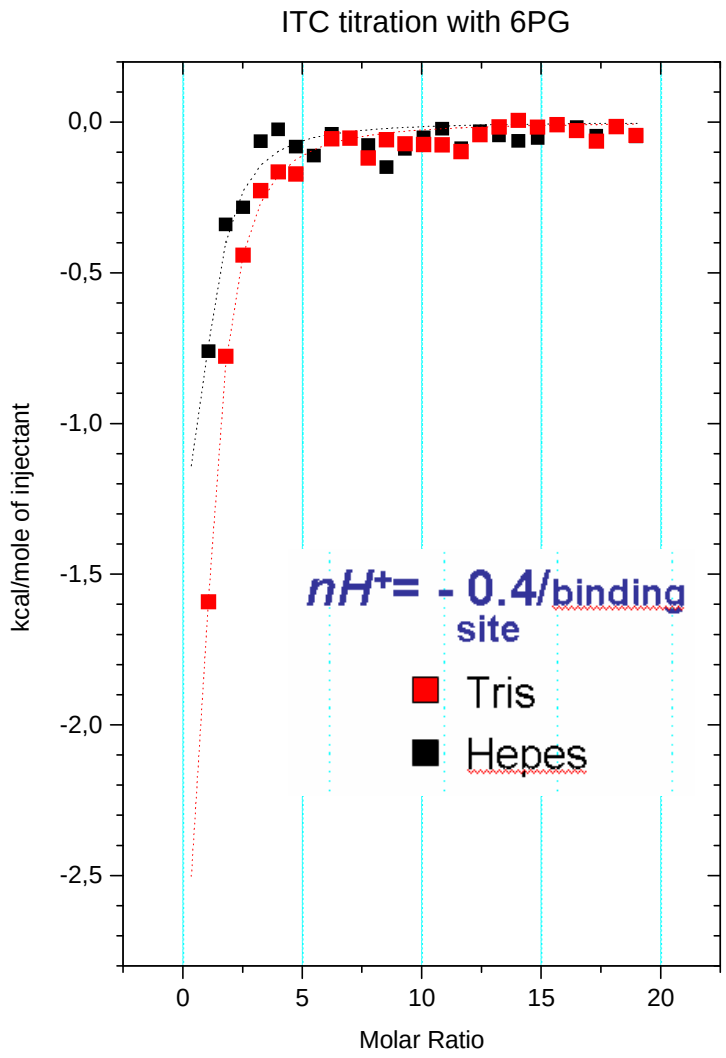

Fig. 17. ITC titration with 6PG in two different buffer.

The fact that $\Delta H_{observed}$ is higher in Tris buffer (red) than in Hepes (black) indicates that there is H^+ release from the enzyme. 6PG releases about 0.4 H^+, and this can account for up to 2–3 kcal mol^{-1} if the hydrogen ion is removed from a nitrogen acid. Both 5PR and 4PE release a very small amount of H^+, and so the measured binding enthalpy is not shielded by the cost of proton release. The H^+ release is observed only in the enzyme-6PG complex, indicating that some rearrangement of the enzyme occurs when the substrate binds, whereas inhibitors are not able to induce the same changes. The selective action of the substrate could be correlated with the change in the protonation state of Lys185, the residue involved in the catalytic activity, that is supposed to release H^+ on binding of the substrate (Fig. 2). The hydroxyl group at C2 of 5PR and the carboxylate group of 4PE (Fig.15) correspond to the hydroxyl group at C3 of 6PG, which faces the amino group of catalytic K185 (Fig.2). 5PR does not release H^+, probably because it does not fit the active site in the same conformation of 6PG; indeed, it has an inverted configuration at C2, so that the hydroxyl group could be misaligned to K185. 4PE does not release H^+ either, probably because the negatively charged carboxylate group facing K185 requires a positively charged group (Fig.12). 4PE (and its derivative 4PEX) is a very powerful inhibitor of 6PGDH, and it has been suggested that it might resemble the dienol intermediate. If 4PE binds to protonated K185, the inhibitor resembles more closely the 3-keto intermediate, which has been suggested to be next to K185 in the protonated state (Fig. 12). As discussed below, 4PE strongly affects the binding of both NADP and NADPH, again suggesting that this inhibitor can mimic some features of the 3-keto intermediate.

Enzyme–coenzyme complexes

The binding parameters for NADP, NADPH and aPyADP (a nonoxidizing analogue of NADP, fig.18) are reported in Table 4. A binding isotherm and the fitted data for the binding of aPyADP to the enzyme are shown in Fig.19.

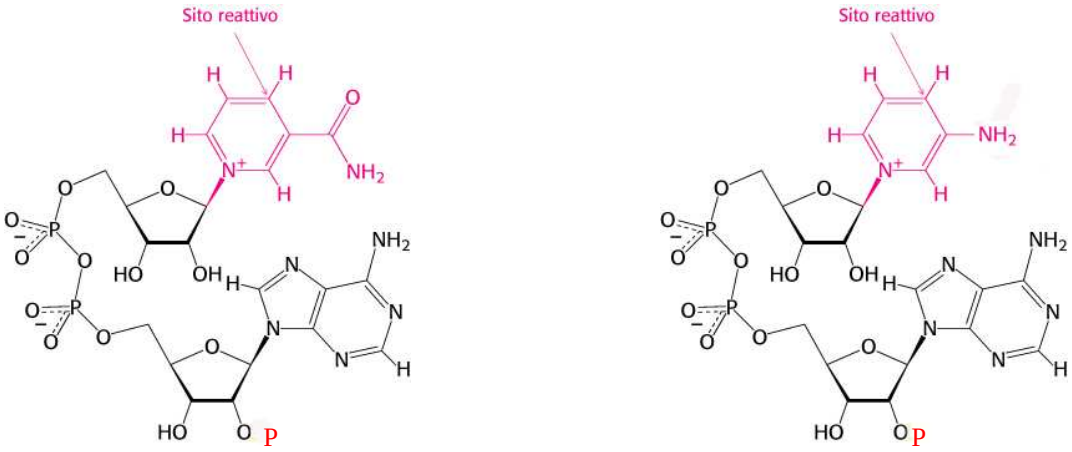

$NADP^+$ **3-Amino pyridine adenine dinucleotide phosphate**

Fig.18. Structures of $NADP^+$ and 3-Amino pyridine adenine dinucleotide phosphate.

Ligand	K_d (μM)	ΔH_0(cal mol^{-1})	$T\Delta S_0$(cal mol^{-1})	nH^+	Sites/dimer
NADP	7.54 ± 0.19	-5382	1486	-0.18	1.86 ± 0.13
NADPH	1.05 ± 0.05	-11819	-3093	0.08	2.07 ± 0.05
aPyADP	1.56 ± 0.1	-10581	-2838	0.45	1.65 ± 0.012

Table 4. Binding parameters of coenzymes to 6PGDH from *Trypanosoma brucei*.

The binding stoichiometry was close to two sites per dimer for all the coenzymes tested. A quite surprising result is the relatively high value of K_d for NADP, around an order of magnitude higher than the K_m value of the coenzyme.

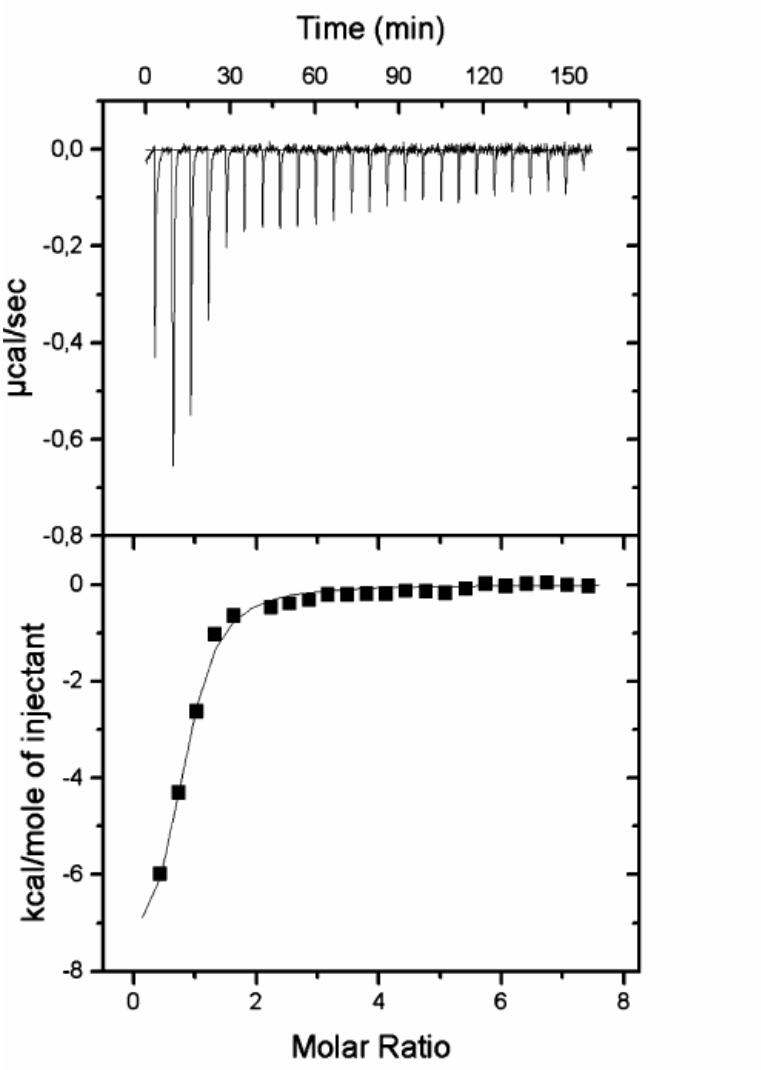

Fig. 19. Titration of *T. brucei* 6PGDH with aPyADP. The cell contained 5.2 µM dimer concentration in 50 mM Hepes buffer at pH 7.5, 0.1 mM EDTA and 1 mM 2-mercaptoethanol. The syringe contained 0.43 mM aPyADP in the same buffer. A total of 25 injections was made at 380 s intervals. Top panel: raw ITC data. Bottom panel: data after the subtraction of the control titration and peak integration. The full line is the fit to a single-site model.

The enthalpy change for NADP binding is relatively low, and a positive entropy change contributes to binding. For NADPH and aPyADP, the binding appears to be totally enthalpic, and a negative entropy change is associated with complex formation. It is known that NADP and NADPH bind in a different way to sheep liver 6PGDH. The differences in the thermodynamic parameters between oxidized and

reduced coenzyme suggest that, also in the *T. brucei* enzyme, coenzyme binding involves different interactions with the protein.

With regard to the thermodynamic parameters, aPyADP resembles more closely NADPH, even though the amino-pyridine ring should be more similar in geometry and charge to that of NADP. Indeed, aPyADP has been used as an analogue of the oxidized coenzyme in 6PGDH from *Candida utilis*. The anomalous behaviour of aPyADP could result from the lack of the carboxamide group (Fig.18), allowing a conformation of the binary complex closer to that of the reduced coenzyme. The different conformation, and the lower steric hindrance, could slightly perturb the pK value of the ionizable groups surrounding the amino-pyridine moiety, resulting in the uptake of 0.45 H^+.

Half-site reactivity of ternary complexes

Titration of the enzyme-6PG complex with aPyADP (Fig. 20) shows a small increase in the dissociation constant of the coenzyme analogue, a more negative binding enthalpy and, more interestingly, a decrease in the binding stoichiometry of the coenzyme (Table 5).

Titrant	**Binary complex**	**K_d (μM)**	**ΔH_0(cal mol^{-1})**	**$T\Delta S_0$(cal mol^{-1})**	**Sites/dimer**
aPyADP	6PGDH-6PG	3.62 ± 0.27	-12645	-5467	1.07 ± 0.08
NADPH	6PGDH-6PG	2.04 ± 0.58	-15670	-8000	1.55 ± 0.064
NADP	6PGDH-5PR	12.9 ± 3.38	-18599	-12273	0.879 ± 0.013
NADP	6PGDH-4PE	0.043 ± 0.04	-15742	-6010	1.0 ± 0.003
NADPH	6PGDH-4PE	0.0203 ± 0.0103	-22299	-12089	1.58 ± 0.09
6PG	6PGDH-aPyADP	10.2 ± 0.7[a]	ND	ND	ND
4PE	6PGDH-NADP	0.177 ± 0.015 1.62 ± 0.062	-8741 -2232	285.6 5601	1.0 ± 0.1 1.0 ± 0.1

Table 5 Ternary complexes of 6PGDH from *T. brucei.* ND, not determined.
[a] From the fluorescence measurements.

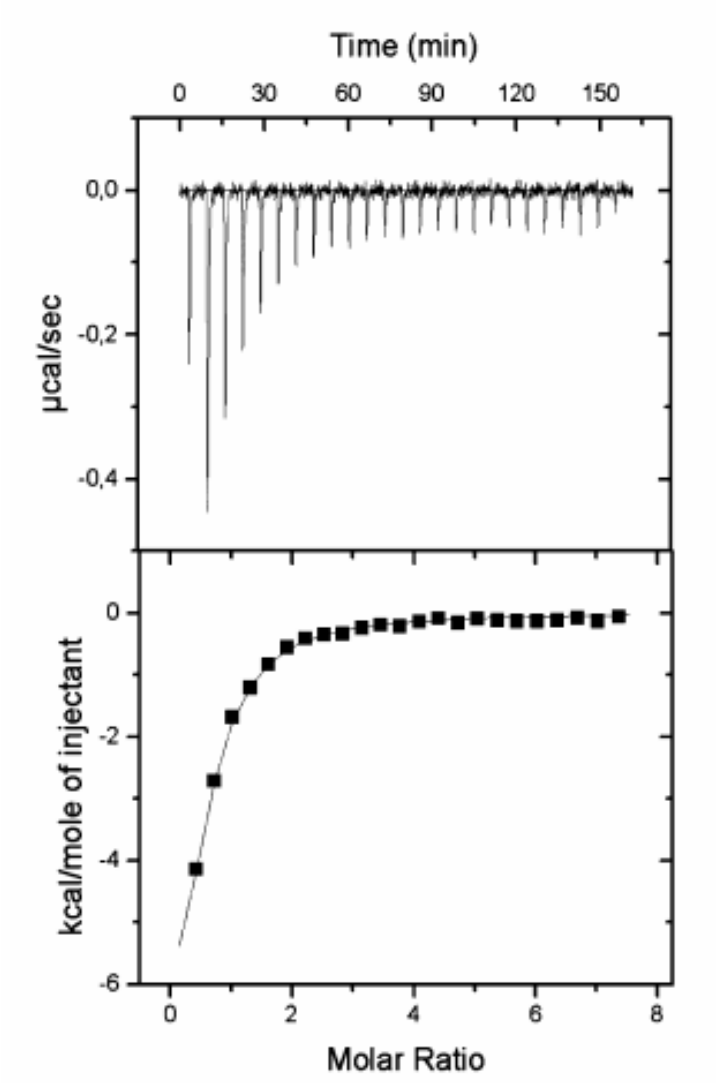

Fig. 20. Titration of the Trypanosoma brucei 6PGDH-6PG complex with aPyADP. The cell contained 5.2 µM dimer concentration and 1.2 mM 6PG in 50 mM Hepes buffer at pH 7.5, 0.1 mM EDTA and 1 mM 2-mercaptoethanol. The syringe contained 0.43 mM aPyADP and 1.2 mM 6PG in the same buffer. A total of 25 injections was made at 380 s intervals. Top panel: raw ITC data. Bottom panel: data after subtraction of the control titration and peak integration. The full line is the fit to a single-site model.

Indeed, only one coenzyme molecule per enzyme dimer is bound. Titration of the same enzyme-6PG complex with NADPH gives a stoichiometry of 1.55 coenzyme molecules per dimer, a value similar to that observed in binary complexes, which

could be accounted for by the partially inactivated enzyme. Thus, the differences between aPyADP and NADPH binding reflect a real change in the stoichiometry.

Titration with NADP of the binary complexes of the enzyme with the inhibitors 5PR or 4PE again shows a binding stoichiometry of about one coenzyme molecule per dimer, confirming the presence of half-site reactivity. Likewise, for 4PE, the binding stoichiometry of NADPH is 1.58 coenzyme molecules per dimer, indicating that the half-site reactivity is strictly limited to the oxidized coenzyme.

To test whether the half-site reactivity involves only the coenzyme, or both NADP and substrate, 6PGDH was titrated with 6PG and 4PE in the presence of saturating concentrations of aPyADP and NADP, respectively. The titration of the enzyme–aPyADP complex with 6PG gives small signals, whose values are so close to blank titrations that it is impossible to handle the experimental data. As binding stoichiometry suggests that only one coenzyme molecule per dimer is bound in the ternary complex, titration of the enzyme-$(aPyADP)_2$ complex with 6PG should cause the release of a coenzyme molecule from the dimer (Fig. 21, step 4). aPyADP release has a large positive ΔH value and is accompanied by H^+ release (Table 4). 6PG binding has a small positive ΔH value and is accompanied by H^+ release (Table 3). Thus, during the formation of the enzyme-6PG-aPyADP ternary complex from the enzyme-$(aPyADP)_2$ complex, there are two opposite effects: a positive ΔH value for aPyADP release and 6PG binding, and a negative ΔH value for buffer protonation. These opposite effects can result in an experimental value close to blank data.

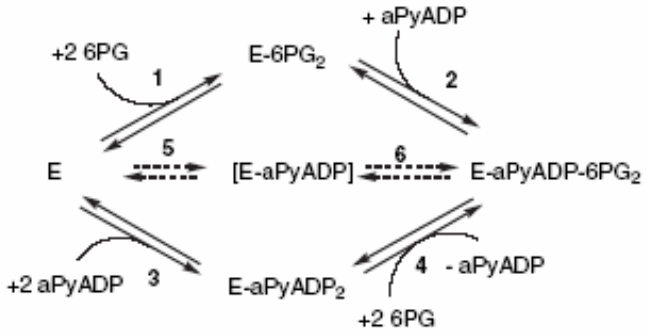

Fig. 21. Kinetic mechanism of the binding to 6PGDH of the substrate 6PG and the NADP analogue aPyADP. The enzyme is a homodimer with a NADP half-site reactivity in the presence of 6PG.

To further study the binding of 6PG to the enzyme-aPyADP complex, we measured the changes in the fluorescence of the bound coenzyme on addition of 6PG (Fig. 22). The fluorescence changes cannot be fitted with a simple binding isotherm; however, the data are consistent with the mechanism depicted in figure 15, where the substrate does not bind to the enzyme-$(aPyADP)_2$ complex. The resulting K_d value, 10.2 ± 0.7 μM (Table 5), is close to 7.81 μM, the value calculated on the basis of multiple equilibrium constraints:

$$K_{6PG4} = K_{6PG1}\, K_{aPyADP2}/K_{aPyADP3}$$

where the numbers in the subscripts refer to the steps in Figure 21.

Further support for the half-site model for *T. brucei* 6PGDH comes from enzyme kinetics. Indeed, although at high 6PG concentrations the enzyme displays the usual Michaelis-Menten kinetics towards NADP, at low 6PG concentrations the enzyme shows a marked inhibition by NADP (Fig.23).

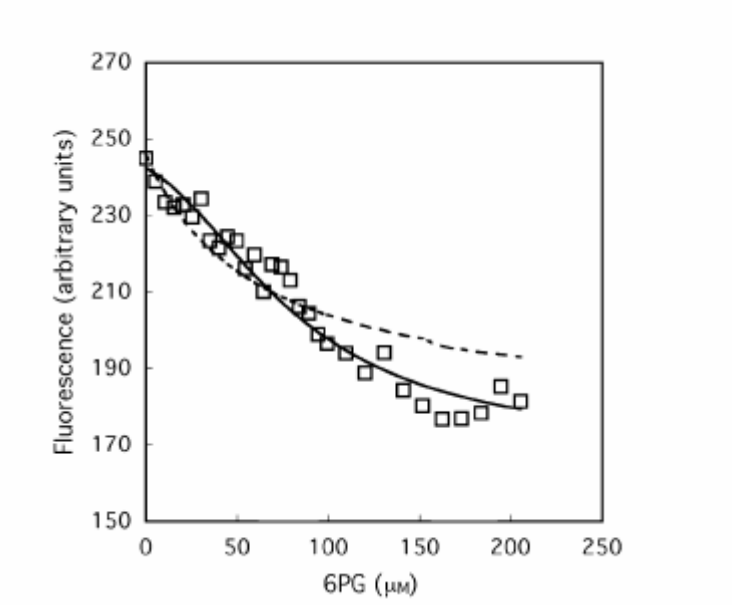

Fig. 22. Fluorescence titration of the 6PGDH–aPyADP complex with 6PG. Changes in the fluorescence of the bound coenzyme on addition of 6PG are shown. Lines were obtained by nonlinear least-squares fitting to a full-site model (broken line) or a half-site model (full line).

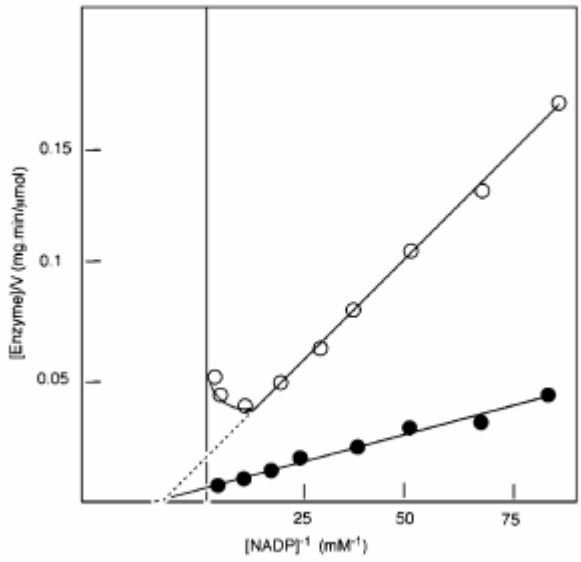

Fig. 23. Inhibition of *T. brucei* 6PGDH by NADP. The assay mixture contained 1 mL of 50 mM triethanolamine buffer, pH 7.5, 1 mM EDTA, 1 mM 2-mercaptoethanol, NADP at the concentration indicated on the abscissa and either 20 μM 6PG (open circles) or 2.2 mM 6PG (filled circles).

This substrate-dependent inhibition by the coenzyme has been observed previously for the enzyme from *C. utilis*, and has been correlated with the presence of half-site reactivity. At low substrate concentrations, the coenzyme inhibits the enzyme by

shifting the equilibrium towards the non productive enzyme-$(NADP)_2$ complex that cannot bind the substrate. At high substrate concentrations, the equilibrium is shifted towards the enzyme–substrate complex, preventing the binding of the second coenzyme molecule, and the inhibition is cancelled [36].

In conclusion, titration of the enzyme-aPyADP complex with 6PG [by both isothermal titration calorimetry (ITC) and fluorescence measurements], titration of the enzyme-6PG complex with aPyADP and kinetic data all support the half-site reactivity of *T. brucei* 6PGDH, where only one ternary complex can be formed on the enzyme dimer.

The binding of 4PE to the enzyme-$(NADP)_2$ complex gives a large measurable enthalpy change, and the best fit is obtained by assuming two sequential binding sites. The first site shows an apparent K_d value of 0.177 μM, very close to the K_i value of the inhibitor determined kinetically (0.18μM) [49]. However, K_2 in Figure 21 must be given by the product K_3K_4/K_1, which is 0.015 μM, much lower than the measured K_d value. To explain this discrepancy, it should be considered that only one NADP molecule can be present in the ternary complex (Table 5), so that, in the formation of the ternary complex, the excess of NADP could act as a competitive inhibitor of 4PE (Figure 21, step 5). In other words, NADP could act as an inhibitor for 4PE binding in the same way as NADP inhibits enzymatic activity. If this holds true, the K_d value measured experimentally is an apparent dissociation constant, and the true value should be obtained by correcting the experimental value by the usual term $K_{app}= K_d(1 + [I]/K_i)$, where I is NADP and K_i is the dissociation constant of NADP for the free enzyme. In our experimental conditions, the calculated true K_d value is 17.7 nM, in good agreement with the value imposed by multiple equilibrium constraints.

The second site shows K_d and ΔH values close to those of the binary complex, suggesting that the asymmetric form of the enzyme causes only moderate effects on the substrate binding site of the subunit devoid of the coenzyme. Thus, the

asymmetric ternary complex binds only one NADP molecule, but still binds two substrate molecules.

The half-site reactivity of 6PGDH has been observed previously in the enzyme from *C. utilis* and from sheep liver. In both cases, the evidence was obtained using an inhibitor derived from NADP, periodate-oxidized NADP [29,30]. Further support for an asymmetric functional enzyme has been obtained by studying the binding of aPyADP in the presence of 6PG [36], and by observing that 6PG enhances the decarboxylation of 3-keto-2-deoxy 6PG, an analogue of the putative intermediate 3-keto 6PG [65,34,35]. Recently, the crystallographic structure of the ternary complex of *L. lactis* 6PGDH with NADP and 4PEX⁄4PEA has been published, showing only one subunit filled by both coenzyme and inhibitor [27]. The superimposition of the subunit bearing NADP and the inhibitor on the other subunit shows a movement of the cofactor binding domain, resulting in a 5° rotation and a 0.7 Å translation, indicating a structural change on one subunit when the other is filled by the ternary complex [27].

Here, we have shown by direct binding experiments that 6PGDH from *T. brucei* also makes only one ternary complex per dimer. In conclusion, the half-site reactivity appears to be common behaviour for 6PGDH.

Substrate analogues and transition state analogues

The ternary complexes formed by aPyADP and 6PG or NADP and 5PR are very similar. Indeed, although the binding enthalpy of the coenzymes is higher in ternary complexes than in binary complexes, the enthalpic gain is compensated by a large entropy loss, and K_d changes slightly (Tables 4 and 5). The large entropy decrease could be a consequence of the tighter binding that reduces the conformational freedom of the residues interacting with the ligands [66].

The fact that the K_d value of 5PR is close to the inhibition constant (Table 3) suggests that 5PR is simply a substrate-competitive inhibitor.

Quite different behaviour is observed for the ternary complexes with 4PE, where the K_d values of NADP and NADPH show a dramatic decrease. In these complexes, the enthalpy gain overcomes the entropy loss as a result of the tighter binding.

In *L. lactis* 6PGDH, an overlay of 4PEX with 6PG and Ru5P indicates that the inhibitors adopt similar conformation in the active site [27]. However, 4PEX lacks the three hydrogen bonds formed by the carboxylate group of 6PG; nevertheless, the K_i value is far below the K_d value of the substrate. The very tight binding of 4PEX can be explained by suggesting that the planar nature of the hydroxamate group should mimic the planar structure of the dienol intermediate (Fig. 21). It is reasonable that 4PE adopts a conformation similar to that of 4PEA, with a water molecule bridging the carboxylate O1 to the catalytic E192 [27,54](Fig. 24).

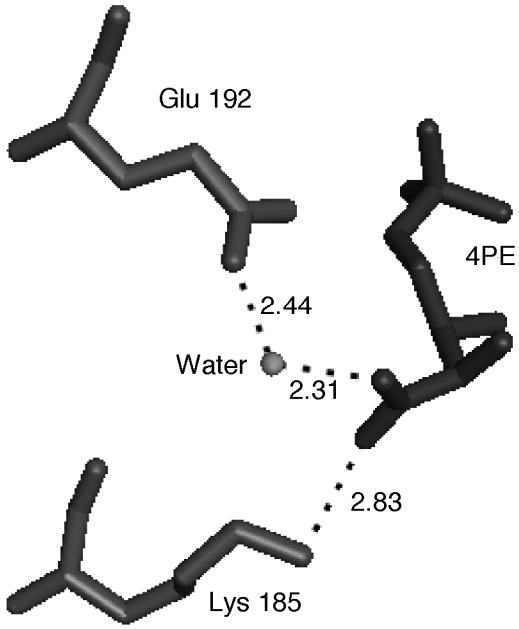

Fig.24. Model of the 4PE bound at the active site of *T. brucei* 6PGDH, with only the amino acid residues Lys 185 and Glu 192 shown, based on the reported structure model of the complex of *L. lactis* 6PGDH with PEA [54].

The observation that 4PE strongly affects both NADP and NADPH binding suggests that the inhibitor should mimic an intermediate in the dehydrogenation step, where

the coenzyme structure changes from the oxidized to the reduced form (Fig. 12). Deuterium kinetic isotope effects indicate a non symmetric transition state for the dehydrogenation reaction, suggesting a 'late' transition state [67]. Within this hypothesis, K185 goes from the non protonated form in the reagents to the protonated form in the transition state, together with C3 becoming planar. The negative charge of the carboxylate group of 4PE could force K185 into the protonated form, thus supporting the conformational/charge changes that strengthen the binding of the transition state.

We suggest that 4PE and 4PEX represent the transition state analogues of two different steps: 4PE, dehydrogenation; 4PEX, decarboxylation (Fig. 12).

The results presented here show some important features fruitful for the design of inhibitors specific for *T. brucei* 6PGDH.

The first observation focuses attention on the role of entropy and the phosphate group. The major contribution to the binding energy of 6PG and its analogues comes from entropy and, in particular, from the entropy gain resulting from the desolvation of the phosphate. The bonds formed by the ligand with the enzyme can only counterbalance the positive desolvation enthalpy of the phosphate. Therefore, the design of new inhibitors should firstly preserve the entropy gain.

The second observation is on the proton linkage, an aspect that can escape the analysis of crystallographic structures. Both the proton release and internal rearrangement of the ionic charges can affect negatively the binding enthalpy. By comparing the binding enthalpy of 6PG and 4PE, it appears that, despite 4PE forming a smaller number of hydrogen bonds than 6PG, the binding enthalpy is greater. This can be related to the absence of H^+ loss on binding of the inhibitor. The presence of the charged carboxylate anion of 4PE near K185 strongly suggests that this residue must be charged, whereas the catalytic mechanism requires an uncharged lysine in the complex with 6PG. The transfer of a hydrogen ion from K185 to the medium or to another functional group of the protein could have a high energy cost, which is absent in the binding of the inhibitor. This appears to be the most rational explanation

of the high affinity of 4PE. Therefore, a better understanding of the catalytic mechanism is a prerequisite for the correct design of new inhibitors.

Last, but not least, the transition state involves not only the substrate analogue, but also the coenzyme. In other words, the inhibitor must be more efficient when the coenzyme is present. In the case of 4PE, the K_d value of the inhibitor is close to the K_d value of the substrate, but it decreases by two orders of magnitude in the presence of both oxidized and reduced coenzyme. This means that a powerful inhibition occurs under both normal cellular conditions, when the NADPH/NADP ratio is high, and stress conditions, when NADPH decreases and NADP increases.

Studies on site-directed mutants of *T. brucei* 6-PGDH

As reported in the Introduction section, K185 and E192 (K183 and E190 in the *sl*6PGDH) appear the residues directly involved in the catalysis. These residues have been identified from the 3D structure of the sheep enzyme and from site-directed mutagenesis. The sheep liver enzyme shows the typical bell-shaped activity-pH curve, while the K182R mutant looses the high pK, and the E190Q looses the low pK [16,17]. Thus it was concluded that the bell-shaped curve comes from the ionization of the two residues. However, when these data were published, the same experiments with the *Tb*6PGDH were in progress in our laboratory, and the results were quite different. For this reason we have reinvestigated not only the kinetics of the mutants of *Tb*6PGDH, but also we tried to verify the substrate-induced change in the ionization of the two residues as postulated by the reaction mechanism.

At the beginning three mutants were studied: K185R where lysine is replaced by a more basic residue as arginine, K185H where lysine is replaced by a more acid residue as histidine, and E192Q where the charged glutamate is replaced by a neutral residue as glutamine. Kinetic parameters at pH 7.5 are reported in table 6.

	Wild Type	E192Q	K185R	K185H
A.S.(UI/mg)	30	0.028	0.02	0.032
Km 6PG (uM)	3.5	12	10.6	//
Km NADP (uM)	1	4.5	7.1	//

Table 6. Kinetic parameters of mutants (E192Q, K185R and K185H) and *wt* enzyme.

For the K185H it was not possible to obtain Km values for the substrate and the coenzyme since it has a bi-phasic kinetics and kinetics is not linear at low substrate and coenzyme concentration. All mutations reduced the enzyme oxidative activity by at least three orders of magnitude, indicating that K185 and E192 are really two key residues in the 6PGDH activity. Km values both for 6PG and NADP increase in the mutants compared to the *wt*. In fig.25 their pH curves are reported together with the *wt* one and the pKs obtained from the pH curves are reported in table 7.

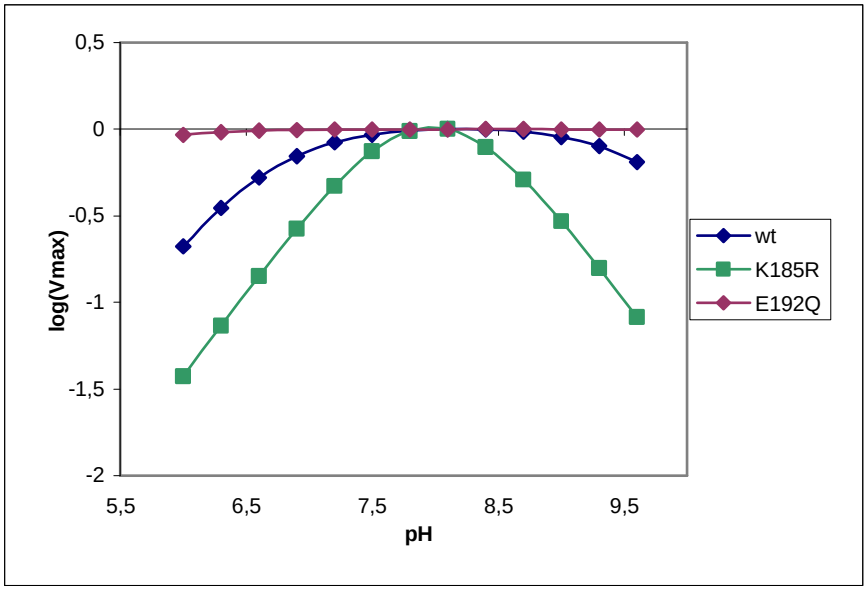

Fig.25. Activity-pH curves. The Y scale is multiplied by an arbitrary factor to allow comparison of the mutant logV with the WT one.

	pKa1	pKa2
WT	6.6	9.8
K185R	7.8	8.15
E192Q	4.9	12

Table 7. pK of K185R, E192Q and *wt*

The *wt* pH curve has the typical bell shape, consistent with the ionization of two residues with pK of 6.6 and 9.8, which, as suggested for the sheep liver enzyme, should be of the glutamate and the lysine. The *T. brucei* mutant curves show a more complicated picture, not similar to that observed for the sheep enzyme, where the lysine or the glutamate mutation causes the loss of one of the two pKs, leaving save the other one. In the *T. brucei* 6PGDH both pKs are perturbed both in the K185R mutant and in the E192Q one. For the K185R the first pK is shifted by 1.2 units toward high pH, while the second pK is down shifted by 1.65 pH units. These data are clearly incompatible with the assumption the higher pK (9.8) observed in the pH curve is the pK of the K185. The same conclusion can be attained for the E192Q, where the first pK is down shifted by 1.7 pH units, and the second pK is up shifted by 2.2 pH units. In conclusion while K185 and Q192 heavily affect the pH curve, other residues are involved.

These results clear the oversimplified model of the pH curve, and open the way to the search on the origin of the shape of the pH curve, whether it comes from other residues involved in the catalytic activity, or from a "global" rearrangement of several unrelated residues induced by conformational changes.

A second question, arising from the experiments on K185R and E192Q mutants, is if the substrate-induced change in the ionization of the two residues postulated by the reaction mechanism is correct.

Two ionisable residues, conserved in all 6PGDH, and not directly involved in the contact with the substrate but within 10 Å of the active site, are H188 and C372.

Two mutants of these residues were prepared, H188L (where histidine is replaced by leucine, a residue with approximatively the same steric hindrance but devoid of acid-base property) and C372S (where cysteine is replaced by an analogue not ionizable residue as serine) to assay the role of H188 and C372.

Residual activity of the H188L mutant is the 4% of the *wt* while is 50% for the C372S (Table 8), while their pH curves (Fig. 26) present alteration of one of the two pKs, the acid for H188L and the basic one for C372S (Table 9).

	Wild Type	**H188L**	**C372S**
A.S.(UI/mg)	30	1.31	16
Km 6PG (μM)	3.5	300	42
Km NADP (μM)	1	n.d	21

Table 8. Kinetic parameters of mutants (H188L and C372S) and *wt* enzyme.
N.d. not determined.

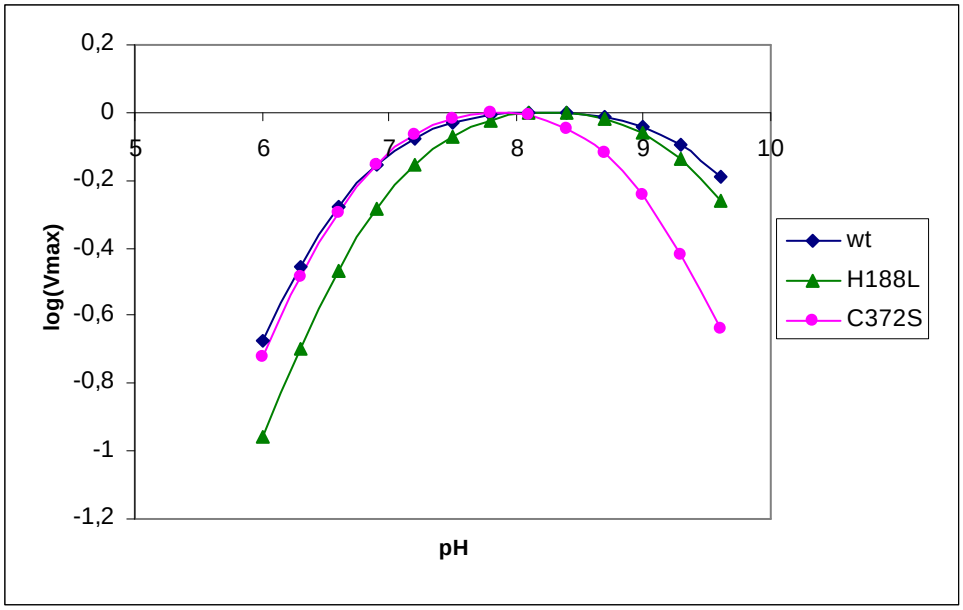

Fig.26. Activity-pH curves. The Y scale is multiplied by an arbitrary factor to allow comparison of the mutant logV with the *WT* one.

	pKa1	pKa2
WT	6.6	9.8
H188L	6.95	9.6
C372S	6.7	9

Table 9. pK of H188L, C372S and *wt*.

The relatively small decrease of specific activity, in particular for C372S, is consistent with a secondary role of these residues in the catalysis. However the changes in the pH curves requires some comments.

The pH curve of the mutant H188L is nearly superimposable at high pH, where the histidine is neutral, while it shows a shift of about 0.4 units at low pH, where the histidine bears a positive charge. This suggests that H188 decreases the pK of some residue(s) contributing to the first pK of the pH curve. In a similar way the curve of the mutant C372S is nearly superimposable at acidic pH, where the cysteine is expected to be neutral, while it shows a shift of about 0.8 units at high pH, where the cysteine bears a negative charge. This suggests that C372 decreases the pK of some residue(s) contributing to the second pK of the pH curve.

These results suggest that the pK observed in the pH curve cannot be attributed to H188 or C372, despite these residues have a role in determining the exact value of the pKs.

It is noteworthy that also the *sl*6PGDH mutants show a very similar behaviour (Fig.27).

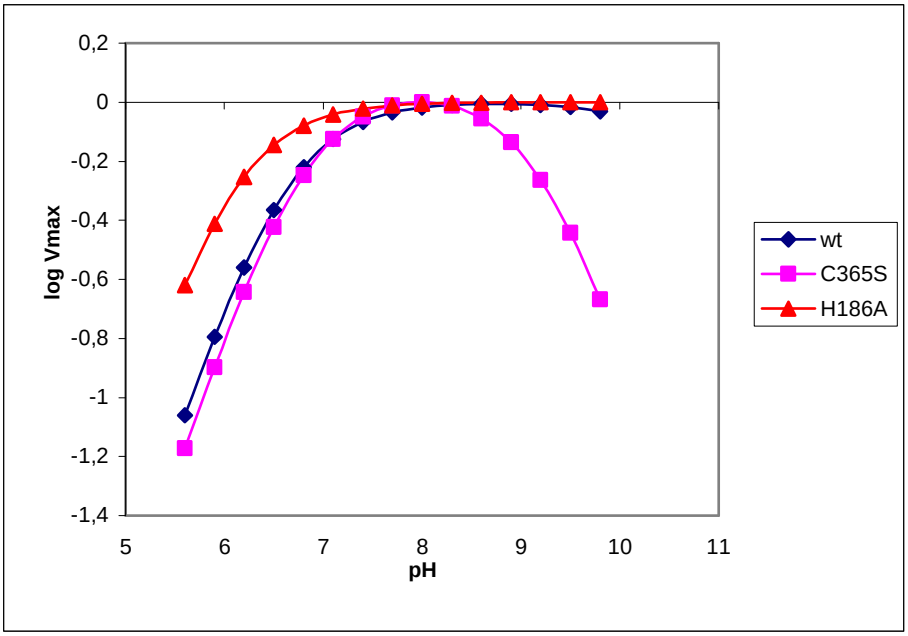

Fig. 27. Activity-pH curves in the sheep liver 6PGDH. The Y scale is multiplied by an arbitrary factor to allow comparison of the mutants (C365S and H186A) logV with the *WT* one.

The pH curve of the H186A mutant is perturbed only at the acidic side of the curve [69], while the C365S mutant is perturbed only at the basic side of the curve (Cervellati, personal communication). However there are significant differences between the *sl* and *Tb* enzymes. The residual activity of H186A is significant (about 15% of the native enzyme), while the residual activity of C365S is only 4%. Also in the pH curve it should be noted that for the H186A mutant the acidic pK is downshifted, while for the corresponding H188L mutant of the *Tb*6PGDH the acidic pK is upshifted. The different behaviour could result from the different steric hindrance in the two mutants. Nevertheless these two residues are involved in the conformational/ionization changes occurring at the substrate binding.

Hydrogen ion movements accompanying the 6PG binding

The proposed reaction mechanism requires that the binding of the substrate changes the ionization state of the two essential residues, K185 and E192, with K185 loosing a H^+ that is taken by E192. To verify this hypothesis we measured by ITC the proton release/uptake occurring on the binding of the substrate.

We firstly studied the *wt* and three mutants: K185H, K185R, and E192Q. Table 10 collect data regarding H^+ exchange between the enzymes and the medium and the ΔH_0 values.

Enzyme	n° H^+	ΔH_0 Kcal/mole
WT	-0.4 ± 0.02	0.174 ± 0.02
K185H	0.78 ± 0.015	-10.08 ± 0.015
K192Q	-1.5 ± 0.023	6.7 ± 0.023
K185R	0	0

Table 10. H^+ exchanged between the enzymes and the medium and the ΔH_0 values at pH 7.5.

The *wild type* 6PGDH upon 6PG binding releases about 0.5 hydrogen ions at all the pH tested (6.5, 7.5 and 8.5), as reported in the previous part of the thesis (fig. 17). The observation that H^+ release is pH independent rules out the contribution of the phosphate group of the substrate to the proton release.

The titration of K185R mutant is indistinguishable from blank titrations at all pH, meaning that the mutant does not exchange H^+ and that the binding enthalpy is zero.

The K185H mutant at pH 6.5 releases about 0.5 H^+, like the *wt* enzyme, while at pH 7.5 and 8.5 the titration in different buffers show that at the formation of enzyme-6PG complex there is capture of hydrogen ions by the medium. Thus at pH 6.5, where the histidine is protonated, there are no differences between *wt* and mutant enzymes, while at higher pH, where the histidine is uncharged, the difference

between wt and K185H mutant is about one hydrogen ion. This suggests that a hydrogen ion coming from the residue 185 is taken up by another enzyme residue. It is noteworthy that for K185H at pH 7.5 the buffer-independent binding enthalpy, ΔH_0, is negative.

If the proposed mechanism is correct, the proton released by K185 should be taken up by E192. In fact the E192Q mutant releases a number of H^+ greater than the *wild type* enzyme at pH 7.5. At pH 8.5 the mutant is unstable and precipitate during the experiment, so at this pH it was not possible to obtain results. For this mutant the value of ΔH_0, is positive.

The calorimetric experiments show that the *wild type* enzyme releases 0.4 H^+ upon 6PG binding. These hydrogen ions can be the result of two different phenomena: 1) an incomplete transfer of only part of the H^+ coming from the lysine to the glutamate with the other released in the medium, or 2) a conformational modification that change the pKa of other ionization groups.

The E192Q mutant brings to exclude the first hypothesis. At pH 7.5 this mutant release 1.49 H^+ (Fig. 28), that is one hydrogen more than *wild type*. This means that the proton transfer of the lysine to glutamate is complete, and the binding of substrate causes structural modification bringing to release of 0.4 protons.

The stoichiometry of the K185H mutant confirms this interpretation. In fact the K185H at pH 7.5, when histidine is non protonated, take 0.78 hydrogen ions. As the histidine pKa is about 6.9, at pH 7.5 the K185H should be in the protonated form for nearly 20%, thus if only a fraction of hydrogen ions should be transferred to the glutamate, the number of H^+ taken from the medium should be lower than 0.3-0.4. The fact that K185H take up 0.78 (Fig. 28) suggests that the proton transfer from lysine to glutamate is complete. In conclusion the calorimetric data show that at the formation of the enzyme-substrate complex, the lysine transfer its proton to glutamate (Fig. 28), at the same time a structure rearrangement on the enzyme causes a release of 0.4- 0.5 protons. In this second process other residues can be involved, the same responsible of the pH effect on the enzyme activity.

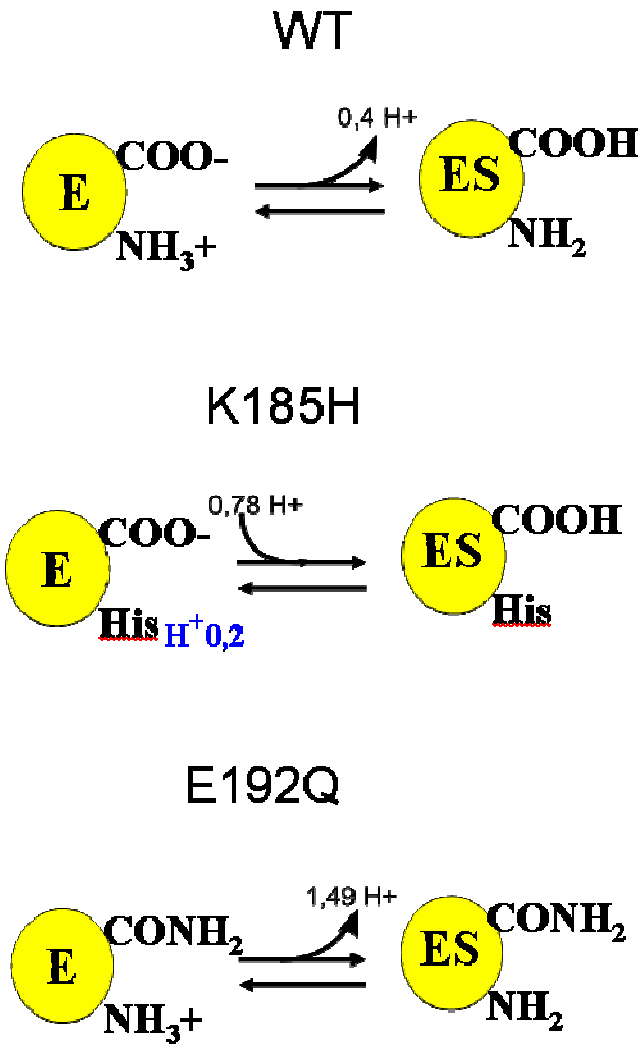

Fig. 28. Scheme of the protonation change in residues 185 and 192 of the wild type enzyme and mutants E192Q and K185H.

The solvent independent binding enthalpy of the three enzymes, *wt*, K185H and E192Q are very different, however if the binding enthalpies are corrected for the ionization costs, the true binding enthalpy appear very similar in all the enzymes. In fact the ionization enthalpy of a lysine or a histidine is about 7-8 kcal mol^{-1}, while the ionization enthalpy of a glutamate is about 1-2 kcal mol^{-1}. If also the hydrogen ion coming from the conformational transition comes from a nitrogen acid, this will add 7-8 kcal mol^{-1}. Taking these values, and the stoichiometry of proton release/uptake, the calculated binding enthalpy for all three enzymes ranges from 8.3 kcal mol^{-1} for

the *wt*, to 7.6 kcal mol^{-1} for the E192Q. These values are very close, and represent the true energy of the bonds between the enzyme and the substrate. However in the *wt* the overall binding energy is less than 0.2 kcal mol^{-1}, while the remaining energy is spent in building up the catalytic machine.

The evidences for a conformational change of the *wt* enzyme, with the release of about 0.5 H^+, let us to investigate the other two mutants; H188L and C372S, to verify whether the moderate effect of these mutation on the enzymatic activity is correlated with the catalysis or with the conformational change.

The binding of 6PG to the H188L mutant show similar ΔH_0 in several buffers and the release in the medium of a very small amount of H^+, about 0.08 (Table 11). This could mean either that the 0.46 H^+ released by the wt come from the H188, or that the mutation of this residue impairs the conformational change reducing the enzymatic activity. As reported in the Introduction section, there are several evidences of a partially rate limiting conformational change of the enzyme-6PG complex, suggesting that the enzyme is shifted from an "open" to a "closed" form (Fig. 29). Kinetic isotope effects of the histidine mutant of the *sl*6PGDH suggest that this residue is involved in the conformational change induced by 6PG. Thus it appears more likely that the lack of proton release observed in the H188L mutant could be due to an impairment of the conformational change.

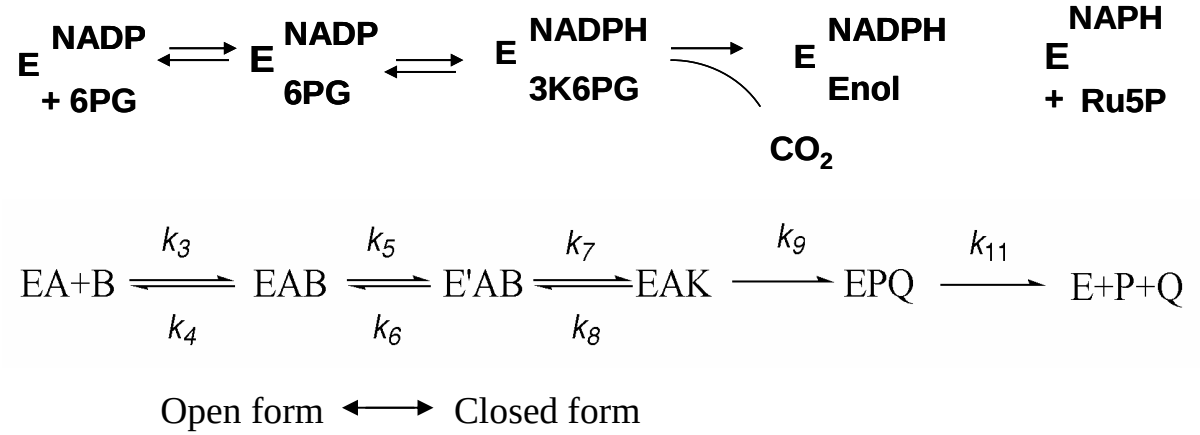

Fig. 29. Isomerisation of the 6PGDH of *T. brucei* enzyme.

Enzyme	n° H^+	ΔH_0 Kcal/mole
WT	- 0.4 ± 0.02	0.174 ± 0.02
H188L	- 0.08 ± 0.016	- 2.9±0.013
C372S	-0.23 ± 0.01	- 1.5±0.012

Table 11: H^+ exchanged between the enzymes and the medium and the ΔH_0 values at pH 7.5.

The C372S mutant release 0.23 proton (Table 11), about one half of the *wt*, and also the activity is one half of that of *wt*. Thus we verified whether there is a correlation between the number of H^+ released and the specific activity.

In figure 30 it is shown a correlation between proton release and enzyme specific for 4 enzyme species: *wt*, K185R, H188L and C372S.

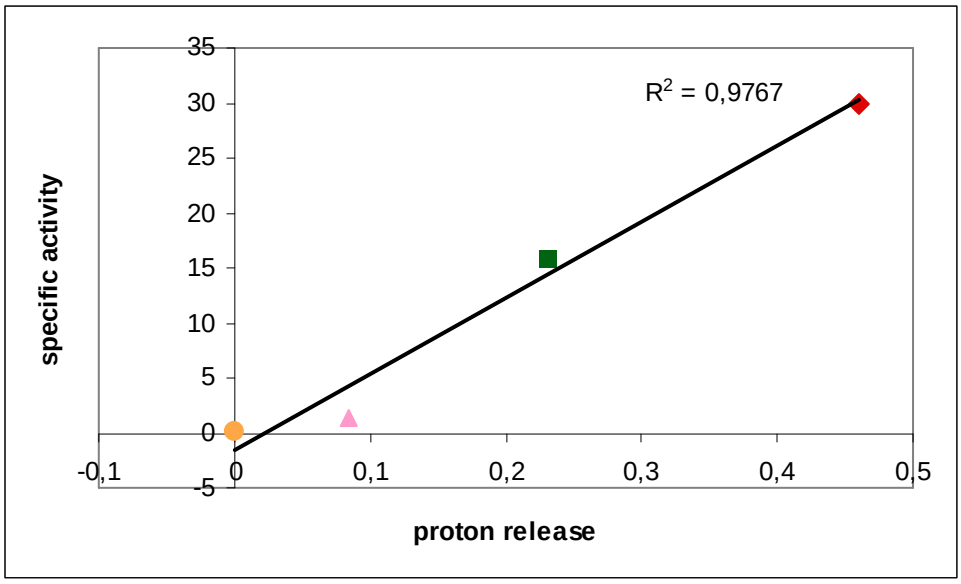

Fig.30. Correlation between proton release and enzyme specific activity, where ● is K185R, ▲is H188L, ■ is C372S and ◆ is *wt*.

Enzyme specific activity and proton release correlate well only for these 4 species while K185H and E192Q, which show a 0.8 H^+ uptake and a 1.5 H^+ release

respectively, do not correlate. This could well be expected since for these two mutants the proton release/uptake is related to the H^+ transfer from K185 to E192, while for H188L and C372S the change in the H^+ release is due to the impaired conformational change upon 6PG binding.

Cysteine reactivity

The conformational changes induced by 6PG binding cause several effects on 6PGDH: increased stability to heat, denaturants, proteolysis, and a dramatic reduction of the reactivity toward chemical modifications. One of the best characterised effects, observed in 6PGDH from several sources, is the loss of reactivity of cysteine residues. Thus we have measured the effect of 6PG on the reactivity of the *Tb* 6PGDH mutants.

In the *T. brucei wild type* 6PGDH, three cysteines for subunit are fastly titrated by DTNB a pH 7.5, but in presence of 6PG one cysteine alone is titrated in more than 10 minutes (Fig.31). In absence of 6PG one cysteine is also more reactive than the others. This behaviour seems in agreement with an open form of the enzyme and a closed more rigid form in the presence of 6PG.

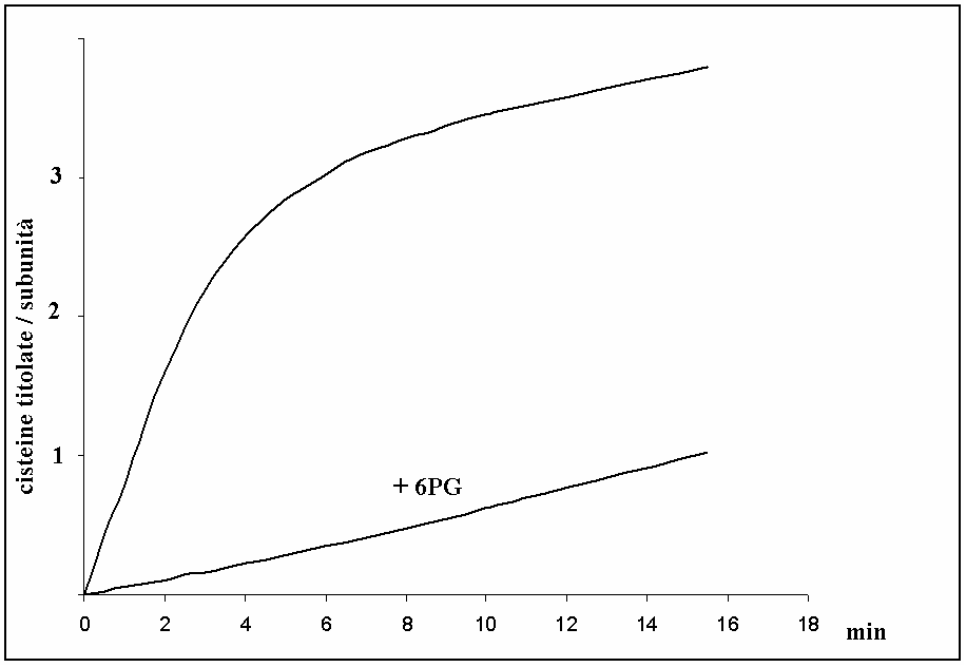

Fig. 31. Cysteine reactivity in the *T. brucei* 6PGDH in presence and absence of 6PG.

This phenomenon has been observed in different species, and in the sheep liver enzyme the most reactive cysteine is cysteine 365 (Cervellati, not published data). This cysteine (cys 372 in the *T. brucei* enzyme) is conserved in all 6PGDHs, and is within 10 Å of the active site. For this reason its ionization, and its reactivity, can be correlated to the ionization state of the residues in the active site.

In the *wild type*, the reactivity of the most reactive cysteine decreases 10-fold in the presence of 6PG (Fig.32).

In the mutant E192Q there is a reduction of reactivity, comparable with that of the *wild type* in the presence of 6PG (Fig.32).

The mutants of the lysine have a different behaviour, in the K185H mutant the cysteine reactivity is reduced compared to the *wild type* both in presence and absence of 6PG, while in the K185R mutant the cysteine reactivity is high in both cases, that is does not change in the presence of 6PG. These data suggest that the 372 cysteine reactivity depends on the ionization state of the residue 185: the cysteine is more reactive if the residue 185 is protonated, while the reactivity decreases if the lysine 185 is not protonated, as it is supposed in the presence of the substrate. The K185H

mutant at pH 7.5 is not protonated even in absence of 6PG, since the pKa of the histidine is 6.9 and in this condition the cysteine reactivity is low. In the K185R mutant, for its higher pKa the arginine is not unprotonated, in the presence of 6PG too. However for K185H and E192Q the proton inventory indicates that, like in the *wt*, the 0,5 H^+ are released in the medium, suggesting that the substrate is able to induce the correct conformational change.

The cysteine reactivity in the C372S and H188L mutants is still high also in the presence of 6PG (Fig. 32) showing that the presence of the two residues C372 and H188 is critical to the shift of the enzyme form the "open" to the "closed" form. Also the K185R mutant, that does not exchange hydrogen ions with the medium, shows the high reactivity of the cysteine residues suggesting an "open" conformation.

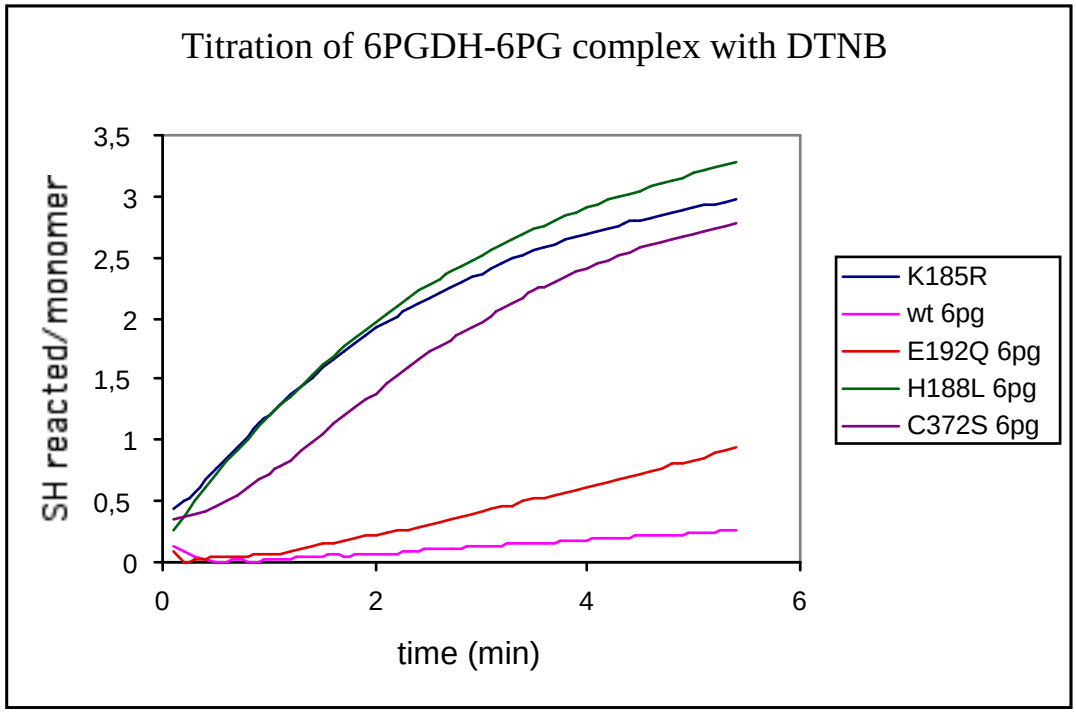

Fig. 32. The cysteines reactivity in absence and in presence of 6PGDH for *wild type*, H188L and C372S.

The initial reaction rates of the cysteine in the presence of 6PG were plotted against the activity of the different mutants (Fig. 33). As already observed for the proton

release, also the reactivity of the cysteines correlates with the activity, suggesting that the loss of activity of the H188L and C372S is due to an impairment of the conformational transition required to put the enzyme in the correct catalytic conformation.

Thus even if H188 and C372 are not directly involved in the substrate binding, they have an important role in the rate-limiting shift of the 6PGDH conformation from the "open" to the "closed" catalitically active form (Fig. 33).

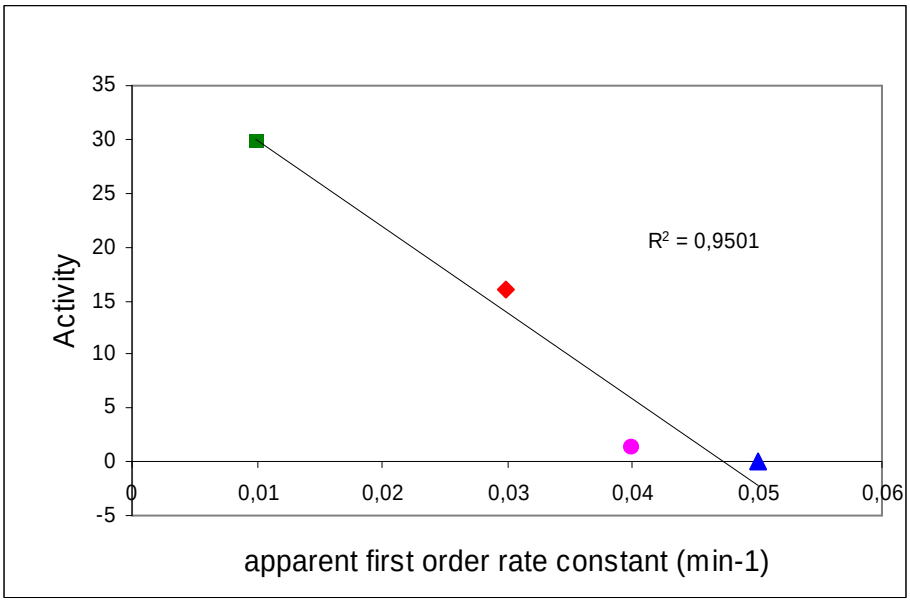

Fig. 33. Initial reactivity of the cysteine residues in the enzyme-6PG complex, where ■ is wt, ◆ is C372S, ● is H188L and ▲ is K185R.

The decrease of enzymatic activity of *Tb* 6PGDH mutants appears to correlate both with the reduced protection of cysteine residues by substrate, and with the number of hydrogen ions released upon substrate binding. This strongly suggests that the substrate induced conformational change plays a key role in the enzymatic activity, as already suggested by kinetic isotope effect studies. Although several residues could be involved in this conformational change, some hypothesis can be drawn on the role of the residues here studied.

As noted above, H188 and to lesser extent C372 are required for a correct conformational transition. However also the K185 mutants appear to have a key function in the transition. In fact K185R does not releases hydrogen ions and does not show 6PG protection of the cysteine residues, meaning that it is unable to allow the transition from the "open" to the "closed" conformation. A closer examination of the K185H suggests that also this mutation affects the conformational change. In fact in K185H the hydrogen ion taken by E190 comes from the solvent (about 0.8 H^+) and from the residual charge of H185 (about 0.2 H^+), meaning that the binding of 6PG does not cause the release of H^+ related to the conformational change. However K185H shows a very low reactivity of the cysteine residues, similar to that of the *wt* enzyme-6PG complex, both in the presence and in the absence of 6PG, suggesting that this mutant is in a conformation similar to the "closed" one also in the absence of the substrate.

The binding of 6PG to the *Tb* 6PGDH involves a large energy change, and the enthalpy contribution to the binding is spent in transferring a hydrogen ion from K185 to E190, and in a conformational change required to put the enzyme in the catalytically competent conformation. This conformation requires that the residue 185 should be uncharged, as suggested by the different behaviour of K185H and K185R. Other residues, H188 and C372, are at different extent involved in the conformational change. The catalytically active conformation is probably retained until the end of the reaction, in fact the complex with the transition-state analogue 4PE shows the same reactivity of the cysteine residues observed in the enzyme-6PG complex, and the catalytic mechanism suggests a charged K185, and proton inventory data are consistent with the retention of the hydrogen ion on K185.

The conformational transition induced by 6PG is a prerequisite for the further conformational changes that affect the coenzyme binding site. In fact in the presence of 6PG the enzyme shows the half-site reactivity toward $NADP^+$. The relevance for the catalytic mechanism of the change from the half-site conformation to the full site

conformation is still elusive. In fact 4PE, that shows all the features of a reaction intermediate, induces half-site reactivity with $NADP^+$ but full site reactivity with NADPH.

PART II

The reverse reaction of 6PGDH studied by kinetic isotope effects

Hydrogen exchange between Ru5P and water

The kinetic mechanism of the reverse reaction of 6PGDH can be described as follow:

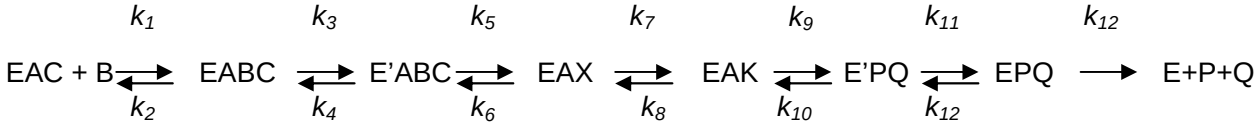

were A is NADPH, B Ru5P, C is CO_2, P and Q are 6PG and NADP respectively. X stays for the enol form of Ru5P and K for the 3K6PG.

Two enzyme isomerisation steps, k_3/k_4 and k_{11}/k_{12} have been inferred on the basis of the results reported below (k_3/k_4) and on the published data (k_{11}/k_{12}) [74,75].

The first step of the reductive carboxylation of Ru5P to 6PG catalysed by 6PGDH is the conversion of Ru5P into a dienol, with the release of the *proR* hydrogen of Ru5P. This reaction requires the presence of NADPH but occurs even in the absence of CO_2, and the hydrogen is exchanged with the medium [14,76] . Therefore we firstly studied the kinetic isotope effects on the exchange reaction.

We measured the rate of hydrogen exchange between Ru5P-*1-h* and Ru5P-*1-d* and tritiated water. The rates of tritium uptake were 0.128±0.004 µmoles min^{-1} mg^{-1} for Ru5P-*1-h* and 0.131±0.004 µmoles min^{-1} mg^{-1} for Ru5P-*1-d*, with a v_H/v_D 0.98±0.06. Furthermore the rate of tritium release from Ru5P-*1-t*, 0.129±0.06 µmoles min^{-1} mg^{-1}, is the same of the tritium uptake from Ru5P-*1-h*. The v_H/v_D ratio is very close both to unity and to the equilibrium isotope effect. This means that C-H breaking is not rate limiting and either deuterium (or tritium) equilibrates freely with the solvent or the

hydrogen ion is shielded from the solvent and the exchange is a side reaction not affected by the isotopic substitution.

The rate of tritium release is low and increases by about one order of magnitude when measured in the reverse reaction. This suggests that either the hydrogen exchange is a side reaction or the presence of CO_2 increases the rate of hydrogen release from Ru5P. To verify whether CO_2 plays a direct role in the proton abstraction from Ru5P, we studied the rate of tritium exchange in the presence and in the absence of CO_2 by using as coenzyme the 1,6NADPH, a non-reducing analogue of NADPH. This analogue can replace the natural coenzyme in the tritium exchange and in the decarboxylation [73]. Our experiments show that the presence of CO_2 does not modify the rate of tritium release from Ru5P-*1-t*, ruling out any role of CO_2 in the first step of the reaction.

The low rate of hydrogen exchange in the absence of the full reverse reaction, and the lack of isotope effect observed in the exchange reaction, both suggest that this is a side reaction that cannot modify at significant extent the isotopic composition of Ru5P during the measurements of the isotopic effects on the reverse reaction.

Kinetic isotope effects on the reductive carboxylation.

The tritium isotope effect on the V/K_{Ru5P} in the reverse reaction of 6PGDH was calculated from the heavy isotope enrichment (equation 3). However the calculated isotope effect appears to increase by increasing the extent of the reaction (Fig. 34). This result is surprising, in fact the presence of an hydrogen exchange occurring independently from the reductive carboxylation should eventually decrease the measured isotope effect. Because the main change occurring during the $^{T}(V/K)$ measurements was the build up of the 6PG in the reaction mixture, we measured the deuterium isotope effects in the reverse reaction both in the presence and in the absence of 6PG. In the absence of 6PG $^{D}(V/K)$ and $^{D}(V)$ were 1.68 and 2.46

respectively. A ^{D}(V/K) lower than ^{D}(V) means that c_{fV} is lower than c_f (eq. 9 eq.7), and from the definition of the commitment factors (eq. 6 eq.4) it follows that

$1/k_4 > (1/k_7 + 1/k_9 + 1/k_{11})$ (11)

This means that all the steps following the proton abstraction from the Ru5P are faster than the release of Ru5P or, in other word, that the chemical steps and the 6PG release are not rate limiting.

In the presence of 40 µM 6PG ^{D}(V/K) increases and ^{D}(V) decreases (2.84 and 1.38 respectively). The increase of ^{D}(V/K) correlates with the observed increase of ^{T}(V/K) when 6PG accumulates in the reaction mixture. A ^{D}(V/K) > ^{D}(V) means that the relation 11 is reversed, and that the presence of 6PG changes the rate limiting step of the reaction.

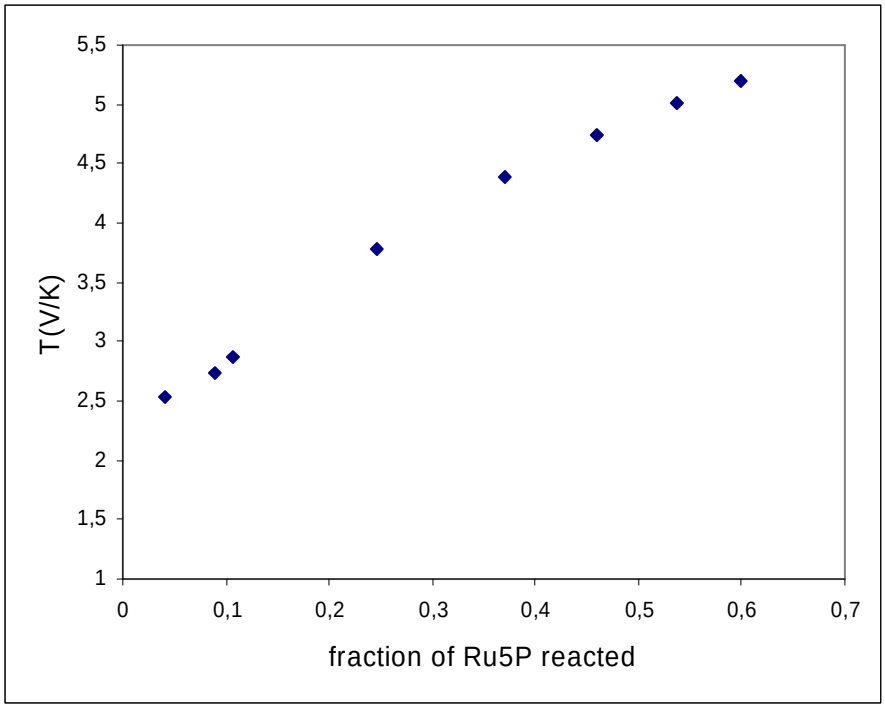

Fig. 34. Tritium isotope effect on the V/K_{Ru5P} in the reverse reaction of 6PGDH

Inhibition of the reductive carboxylation by 6PG

6PG is known as competitive inhibitor toward Ru5P in the reverse reaction of the 6PGDH. We have reinvestigated the inhibition by 6PG, and we observed that at low concentration the inhibitor slightly increases the rate of the reaction. At higher concentrations 6PG behaves as a conventional competitive inhibitor (Fig. 35), with a K_i 9.3 µM, but back extrapolation of the enzyme activity to zero 6PG give an enzymatic activity about five fold higher than the activity really measured.

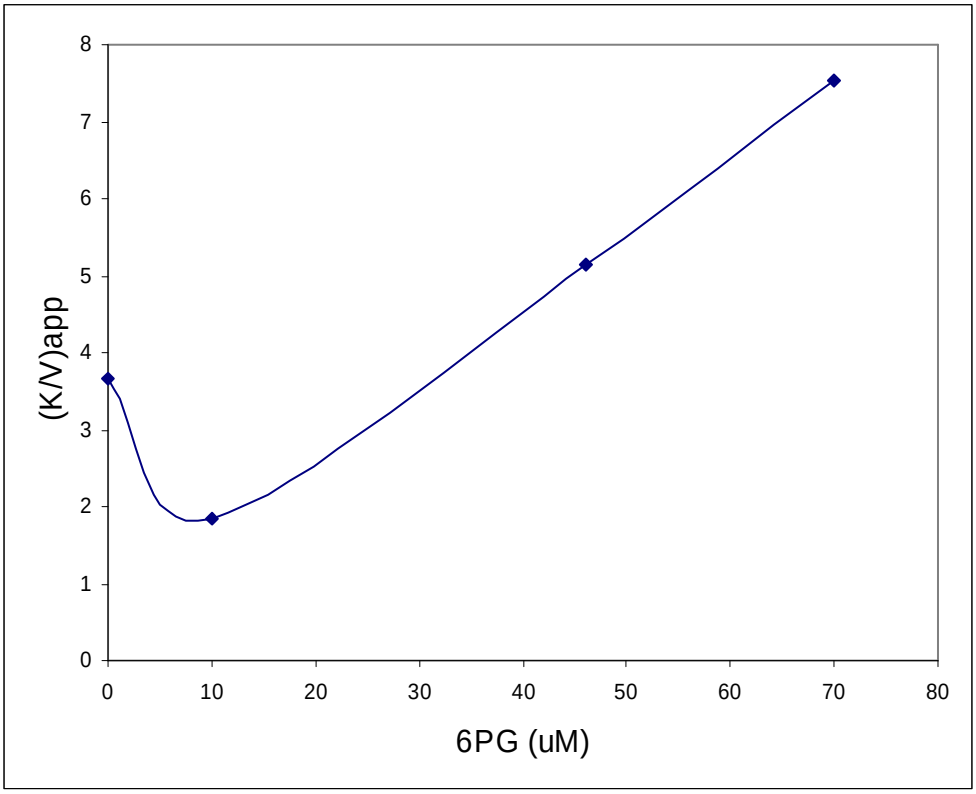

Fig. 35. Effect of 6PG on the reductive carboxylation by *C. utilis* 6PGDH.

These data suggest that 6PG has a double effect: it activates the reverse reaction, probably by removing a rate limiting step, and inhibits the reaction by competing with the Ru5P.

The effect of 6PG on the reverse reaction of 6PGDH was totally unexpected. At relatively high concentrations 6PG behaves as classical competitive inhibitor. However at low concentrations of 6PG, when the two subunits of the dimer are occupied at the same time by 6PG and Ru5P, the enzymatic activity increases, meaning that when 6PG is bound to one subunit, the catalytic activity of the other subunit increases. These results can be correlated with the previously reported observation that 6PG increases the rate of decarboxylation of the 3-keto-2-deoxy-6PG (3Kdo6PG), an analogue of the putative reaction intermediate 3-Keto-6PG. 6PGDH from sheep liver does not decarboxylate the 3Kdo6PG, but 6PG is able to induce the decarboxylation even in the absence of coenzymes [34]. Also for 6PGDH from other sources, that slowly decarboxylate the 3Kdo6PG, the presence of 6PG increases the rate of decarboxylation by over one order of magnitude [35]. Taking together the old and the new evidences it appears clearly that the maximum efficiency in the catalytic reaction requires a 6PG bound to one subunit, while the catalysis occurs at the other subunit.

As reported above, in the absence of 6PG the deuterium isotope effects indicate that k_4 is the slowest step, meaning that in the forward reaction (from 6PG to Ru5P) the product release should be rate limiting. This result is conflicting with the previously reported data [74] showing that the first steps of the forward reaction, isomerisation of the enzyme-NADP-6PG complex, dehydrogenation and decarboxylation, are rate limiting. Apparently there is a violation of the principle of microscopic reversibility.

When the isotope effects are measured in the presence of 6PG, despite the inhibition, the value of $^{D}(V/K)$ increases while the value of $^{D}(V)$ decreases, meaning that under

these conditions k_4 is not rate limiting (Table 11). It should be noted that the measurements of the forward reaction are necessarily carried out in the presence of 6PG, therefore when the experiments are carried out under condition more similar to that used for the measurements of the forward reaction the principle of microscopic reversibility is satisfied. This change in the rate limiting steps is confirmed by the change of $^{T}(V/K)$, that increases as the reaction proceeds and 6PG builds up in the reaction mixture.

parameter	isotope effect	
	- 6PG	+6PG
$^{D}(V)$	2.46	1.38
$^{D}(V/K)_{Ru5P}$	1.68	2.84
$^{T}(V/K)_{Ru5P}$	2.55	5.20

Table 11. Deuterium and tritium isotope effect on the reductive carboxylation of Ru5P by 6PGDH.

This could be an effect on the chemical step itself, or on the release of the Ru5P. The possibility that the product release could be rate limiting has never taken into account, because under the usual conditions for initial rate measurements the release of CO_2 is fast and irreversible, and Ru5P has a relatively low affinity for the enzyme.
A more detailed analysis of the isotope effect could show whether the slow step is an isomerisation step, preceding the chemical steps, or also the proton abstraction and/or carboxylation are affected. We can take the tritium isotope effect measured at low substrate conversion as indicative of the $^{T}(V/K)$ in the absence of 6PG, and the isotope effect measured at high substrate conversion as indicative of the $^{T}(V/K)$ in the presence of 6PG (Table 11). Despite the uncertainty due to the experimental errors in the determination of the deuterium isotope effects and to the change of the tritium isotope effects as the reaction proceeds, for each condition, without 6PG and with 6PG, we have three equation ($^{D}(V)$, $^{D}(V/K)$ and $^{T}(V/K)$) with four unknown ($^{D}k_5$, c_f,

c_r and c_{fV}), and an estimate of $^{D}k_5$ can be obtained by setting arbitrary values of c_r in eq 10.

$$\frac{^{D}(V/K)-1}{^{T}(V/K)-1} = \frac{^{D}k_5 - 1 + c_r\left(^{D}K_{eq} - 1\right)}{^{D}k_5^{1.441} - 1 + c_r\left(^{D}K_{eq}^{1.441} - 1\right)} \qquad (10)$$

In the absence of 6PG, computer fitting gives a small range of c_r, and when $c_r > 1.6$, c_{fV} becomes negative. Thus from $^{D}(V/K)$ and $^{T}(V/K)$ we obtain a $^{D}k_5$ ranging from 4.90 to 4.92 (Table12). The high values of c_f (3.11-4.76) indicate that k_4 is lower than k_5. The release of Ru5P is thought to be fast [74] so it is unlikely that k_4 could be the Ru5P release step. To explain the low value of c_f a slow step preceding the isotope sensitive step has been inserted in the mechanism. This step is likely an isomerisation of the enzyme-substrate complex, similar to the partially limiting isomerisation observed in the forward reaction [74].

c_r	$^{D}k_5$		c_f		c_{fV}	
	-6PG	+6PG	-6PG	+6PG	-6PG	+6PG
0	4.92	4.94	4.76	1.14	1.68	9.37
1	4.91	4.93	3.73	0.13	0.67	8.34
1.1	4.91	4.93	3.63	0.028	0.57	8.23
1.6	4.90	--	3.11	--	0.071	--

Table12. Calculated values of intrinsic isotope effect and commitment factors.

In the presence of 6PG, the allowable values of c_r are still small, and for $c_r > 1.1$, c_f becomes negative. The calculated values of $^{D}k_5$ are still comprised in a very small range, 4.93 to 4.94. The values of c_f are small (0.028-1.14) showing that either k_4 increased or k_5 decreased. A decrease of k_5 is unlikely, in fact we observed that 6PG increase the reaction rate, thus the main effect of 6PG appears to be on the

isomerisation step preceding the chemical steps. The allowable values of c_r are very close both in the presence and in the absence of 6PG, suggesting that the steps following the proton abstraction are unaffected, or only slightly affected by the presence of 6PG.

Thus $^{D}k_5$ is defined in a narrow range, 4.90-4.94, and poorly affected by the presence of 6PG. This suggests that, despite the caveat above reported on the quality of the experimental data, the overall analysis of the isotope effects gives a reliable picture of the kinetics of the reaction. A deuterium intrinsic isotope effect of about 5 suggests that the transition state symmetry of the catalysed reaction is similar to that of the reaction in solution.

The allowable values of c_r come from several rate constants. Nevertheless an approximate value for the ratios k_6/k_7, k_8/k_9, and k_{10}/k_{11} can be calculated. To do this we can use the values of the commitment factors determined by Cook [74,75] in the study by kinetic isotope effects of the oxidative decarboxylation. It can be easily seen that the c_f and c_r in the oxidative decarboxylation are respectively the ratio k_{10}/k_{11} and k_9/k_8 in the reverse reaction.

In the study of the oxidative decarboxylation only a range of allowable values of c_r and c_f has been determined. To choose a value, we take into account that the ratio of the rates of reduction and decarboxylation of 3K2do6PG [76] is about 1.5. Thus if the observed rates reflect the decarboxylation (k_8) and the reduction (k_9), an appropriate value for the c_r of the oxidative decarboxylation is 0.66. Taking the corresponding value for c_f, we can calculate the k_6/k_7 ratio for the reductive carboxylation:

$$k_6/k_7=(c_r)_{rev} /(1+(1/c_r)_{fw}(1+(c_f)_{fw}))$$

where the subscripts rev and fw refers to the reductive carboxylation and to oxidative decarboxylation respectively.

In conclusion approximate estimate of the ratios between the rate constants can be calculated over the whole reaction pathway, with the exception of the on/off rates of reactants and products. This allows to draw the upper part of the energy profile of the

reaction (Fig. 36), while the lower part requires the knowledge of the steady-state concentrations of the intermediates. It can be seen that in the absence of 6PG the rate limiting step is the isomerisation of the enzyme-Ru5P complex, while in the presence of 6PG the rate limiting step is the isomerisation of the enzyme-6PG complex.

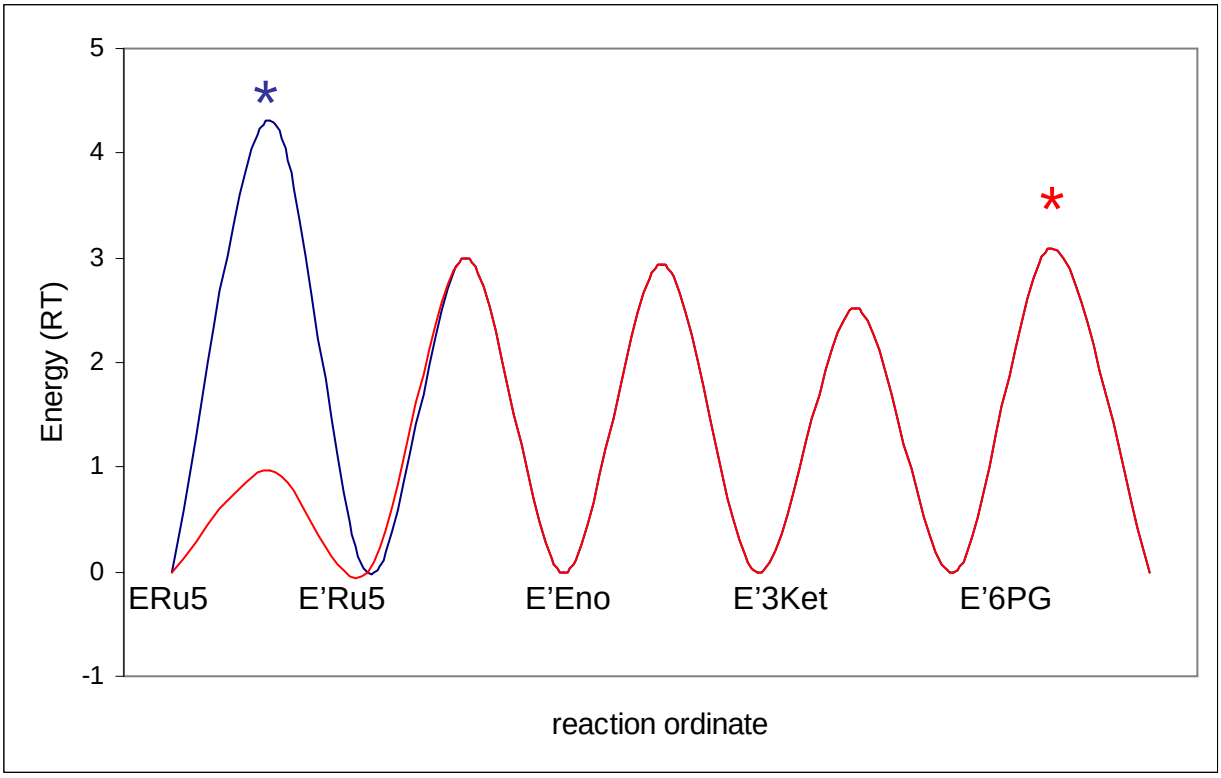

Fig. 36. Energy profile in function of reaction ordinate.

CONCLUSIONS

A common feature of all the experiments here reported is the key role of the conformational changes in the catalytic mechanism of 6PGDH. At least two different conformational changes occur during the catalysis: a first one when the 6PG, or a 6PG analogue, binds to the enzyme. This conformational change requires a large enthalpy increase and involves not only the residues of the active site, but also H188 and C372. A second conformational change occurs during the catalysis, as suggested by the large change of the K_d of 4PE in the presence of the coenzymes. It should be noted that the high inhibition constant of 4PE cannot be observed in the binary complex, meaning that the development of new inhibitors cannot be based only on binding experiments.

The conformational changes are also important in the enzyme kinetics, in fact they are the rate limiting steps of the reaction, both in the forward and in the reverse directions.

BIBLIOGRAPHY

1. Barrett, M. P. **The fall and rise of sleeping sickness,** The Lancet 1999, 353, 1113-4.
2. Barry, J.D.; McCulloch, R. **Antigenic variation in trypanosomes: enhanced phenotypic variation in a eukaryotic parasite**, Adv. Parasitol., 2001, 49, 1.
3. Pepin, J.; Milord, F. **The treatment of human African trypanosomiasis,** Adv. Parasitol., 1994, 33, 1-47.
4. Barrett, M. P. **Problems for the chemotherapy of human African trypanosomiasis,** Curr. Opin. Infect. Dis., 2000, 13, 647-651.
5. Stevens, J.R.; Noyes, H. A.; Schofield, C. J; Gibson, W. **The molecular evolution of Trypanosomatidae,** Adv. Parasitol. 2001, 48,1.
6. Barrett, M. P.; Burchmore, R. J. S.; Stich, A.; Lazzari, J. O.; Frasch, A. C.; Cazzulo, J-J.; Krishna, S. **The trypanosomiases,** The Lancet. 2003 1, 362, 1469-80. Review.
7. Barrett, M. P.; Mottram, J. C.; Coombs, G. H. **Recent advances in identifying and validating drug targets in trypanosomes and leishmanias,** Trends Microbiol. 1999, 7:82-8.
8. Bastin, P.; Sherwin, T.; Gull, K. **Paraflagellar rod is vital for trypanosome motility,** Nature. 1998, 391, 548.
9. Kreiger. S.; Schwarz, W.; Ariyanayagam, M. R.; Fairlamb, A. H.; Krauth-Siegel, R. I.; Clayton, C. **Trypanosomes lacking trypanothione reductase are avirulent and show increased sensitivity to oxidative stress,** Mol. Microbiol. 2000, 35, 542.
10. Aronov, A. M.; Surcsh, S.; Buckner, F. S.; Van Voorhis, W. C.; Verlinde, C. L.; Opperdoes, F. R.; Hol, W. G.; Gelb, M. H. **Structure-based design of submicromolar, biologically active inhibitors of trypanosomatid**

glyceraldehyde-3-phosphate dehydrogenas, Proc. Natl. Acad. Sci. USA. 1999, 96, 4273-8.

11. Barrett, M. P. **The pentose phosphate pathway and parasitic protozoa, Parasitol** Today 1997, 13, 11-6.
12. Cronin, C. N.; Nolan, D. P.; Voorheis, H. P. **The enzymes of the classical pentose phosphate pathway display differential activities in procyclic and bloodstream forms of *Trypanosoma brucei,*** FEBS Lett. 1989, 244, 26-30.
13. Hanau S, Dallocchio F & Rippa M **NADPH activates a decarboxylation reaction catalyzed by lamb liver 6-phosphogluaconate dehydrogenase.** Biochim Biophys Acta 1992, 1122, 275-277.
14. Lienhard GE & Rose IA **The mechanism of action of 6-phosphogluconate dehydrogenase.** Biochemistry 1964, 3, 190-195.
15. Adams MJ, Ellis GH, Gover S, Naylor CE & Phillips C **Crystallographic study of coenzyme, coenzyme analogue and substrate binding in 6-phosphogluconate dehydrogenase: implications for NADP specificity and the enzyme mechanism.** Structure 1994, 2, 651–668.
16. Zhang L, Chooback L & Cook PF **Lysine 183 is the general base in the 6-phosphogluconate dehydrogenase-catalyzed reaction.** Biochemistry 1999, 38, 11231–11238.
17. Karsten WE, Chooback L & Cook PF **Glutamate 190 is a general acid catalyst in the 6-phosphogluconate dehydrogenase-catalyzed reaction.** Biochemistry 1998, 37, 15691–15697.
18. Barrett, M. P., Le Page, R.W.F. **A 6-phosphogluconate dehydrogenase gene from *Trypanosoma brucei*.** Mol. Biochem. Parasitol., 1993, 57, 89-100.
19. Krepinsky, K., Plaumann, M., Martin, W., Schnarrenberger, C. **Purification and cloning of chloroplast 6-phosphogluconate dehydrogenase from spinach.** Eur. J. Biochem., 2001, 268, 2678-2686.

20. Hannaert, V., Saavedra, E., Duffieux, F., Szikora, J.P., Rigden, D.J., Michels, P.A.M., Opperdoes, F.R. **Plant-like traits associated with metabolism of Trypanosoma parasites.** Proc.Natl. Acad. Sci. USA, 2003, 100, 1067-1071.
21. Corpet F., **Multiple sequence alignment with hierarchical clustering,** Nucleic Acids Res., 1988, 16(22). 10881-90.
22. Gouet P., Robert X., Courcelle E., **ESPript/ENDscript : Extracting and rendering sequence and 3D information from atomic structures of proteins**, Nucleic Acids Res, 2003, 31(13) :3320-3323.
23. Emmanuel Tetaud, Stefania Hanau, Jeremy M. Wells, Richard W.F. Le Page, Margaret J. Adams, Scott Arkison & Michael P. Barret, **6-phosphogluconate dehydrogenase from *Lactococcus lactis*: a role for arginine residues in binding substrate and coenzyme,** Biochem. J. 1999, 338, 55-60.
24. Philips, C.; Dohnalek, J.; Gover. S.; Barrett, M. P.; Adams, M. J. **A 2.8 A resolution structure of 6-phosphogluconate dehydrogenase from the protozoan parasite Trypanosoma brucei: comparison with the sheep enzyme accounts for differences in activity with coenzyme and substrate analogues.** J. Mol Biol. 1998, 282:667.
25. Philips, C.; Gover. S.; Adams, M. J. **Structure of 6-phosphogluconate dehydrogenase refined at 2 A resolution,** Acta Crystallogr. D Biol. Crystallogr. 1995, 51;290-304.
26. Adams, M. J.; Ellis, G. H.; Gover, S.; Naylor, C. E.; Philips, C. **Crystallographic study of coenzyme, coenzyme analogue and substrate binding in 6-phosphogluconate dehydrogenase: implications for NADP specificity and the enzyme mechanism,** Structure. 1994, 2:651-68.
27. Sundaramoorthy R.; Iulek J.; Barrett M.P.; Bidet O.; Ruda G. F.; Gilbert I.H.; Hunter W.N.; **Crystal structures of a bacterial 6-phosphogluconate dehydrogenase reveal aspects of specificity, mechanism and mode of inhibition by analogues of high-energy reaction intermediates**, FEBS J, 2007, 274(1) : 275-286.

28. Dyson, J. E. D.; d'Orazio, R. E.; and Hanson, W. H. **Sheep liver 6-phosphogluconate dehydrogenase: isolation procedure and effect of pH, ionic strength, and metal ions on the kinetic parameters**, Arch. Biochem & Biophys. 1973, 154:623-35.
29. Rippa M, Bellini T, Signorini M & Dallocchio F **The stabilization by a coenzyme analog of a conformational change induced by substrate in the 6-phosphogluconate dehydrogenase.** Arch Biochem Biophys 1979, 196, 619–623.
30. Hanau S, Dallocchio F & Rippa M **Subunits asymmetry in the ternary complex of lamb liver 6-phosphogluconate dehydrogenase detected by a NADP analogue.** Biochim Biophys Acta 1992, 1122, 273–277.
31. Topham CM, Matthews B & Dalziel K **Kinetic studies of 6-phosphogluconate dehydrogenase from sheep liver.** Eur. J. Biochem. 1986, 156, 555–567.
32. Dallocchio F, Matteuzzi M & Bellini T **Half-site reactivity in 6-phosphogluconate dehydrogenase from human erythrocytes.** Biochem J 1985, 227, 305–310.
33. Voinova N.E, Chesnokova L.S & Lyzlova S.N, **Negative cooperativity of 6-phosphogluconate dehydrogenase in rat liver.** Biokhimiia 1996, 61, 451–454.
34. Hanau S, Dallocchio F & Rippa M, **Is there an alternating site co-operativity between the two subunits of lamb liver 6-phosphogluconate dehydrogenase?** Biochem J 1993, 291, 325–326.
35. Rippa M, Giovannini PP, Barrett MP, Dallocchio F & Hanau S, **6-Phosphogluconate dehydrogenase: the mechanism of action investigated by a comparison of the enzyme from different species.** Biochim Biophys Acta 1998,1429, 83–92.

36. Dallocchio F, Matteuzzi M & Bellini T **Effect of the substrate on the binding of coenzyme and coenzyme analogues to 6-phosphogluconate dehydrogenase from Candida utilis**. J. Biol. Chem. 1981, 256, 10778-10780.
37. Berdis A. J. e Cook P. F. **The 2'-phosphate of NADP is critical for optimum productive binding to 6-phosphogluconate dehydrogenase from Candida utilis,** Arch. Biochem. Biophys. 1993, 305, 551-558.
38. Rippa M., Signorini M. e Pontremoli S. **Purification and properties of two forms of 6-phosphogluconate dehydrogenase from Candida utilis.** Eur. J. Biochem., 1967, 1, 170-178.
39. Rippa M., Signorini M. e Pontremoli S. **Evidences for the involvement of a histidine residue in the binding of the substrate to the 6-phosphogluconate dehydrogenase,** Arch. Biochem. Biophys., 1972, 150, 503-510.
40. Dallocchio, F., Signorini M. Rippa M., **Evidence for the proximity of a cysteinyl and a tyrosyl residue in the active site of 6-phosphogluconate dehydrogenase,** Arch. Biochem. Biophys., 1978, 185, 57-60.
41. Rippa M., Signorini M. and Dallocchio, F., **Evidence for the proximity of two sulfhydryl groups at the active site of 6-phosphogluconate dehydrogenase,** Arch. Biochem.Biophys., 1978, 186, 406-410.
42. Rippa M., Signorini M. Bellini, T. and Dallocchio, F., **The active site of 6-phosphogluconate dehydrogenase. A phosphate binding site and its surroundings,** Arch. Biochem.Biophys. 1978, 189, 516-523.
43. Rippa M., Signorini M. and Bellini T, **The effect of inorganic phosphate on the stability of some enzymes,** Biochem. J., 1981, 197, 747-749.
44. Hanau, S., Dallocchio, F. and Rippa, M. **Use of trinitrobenzensulfonate for affinity labeling of lysine residues at phosphate binding sites of some enzymes,** Arch. Biochem.Biophys. 1993, 302, 218-221.
45. Hanau, S., Dallocchio, F. and Rippa M, **Subunits asymmetry in the ternary complex of lamb liver 6-phosphogluconate dehydrogenase detected by a NADP analogue,** Biochem. Biophys. Acta, 1992, 1159, 262-266.

46. Hanau, S., Rinaldi, E., Dallocchio, F., Gilbert, I. H., Dardonville, C., Adams, M.J., Gover, S., Barrett, M.P. **6-phosphogluconate dehydrogenase: a target for chemotherapy in African trypanosomiasis.** Curr. Med. Chem., 2004,11, 1345-1359.
47. Barrett, M.P., Gilbert, I.H. **Perspectives for new drugs against Trypanosomiasis and Leishmaniasis.** Curr. Top. Med. Chem., 2002, 11, 3205-3214.
48. Dardonville, C., Rinaldi, E., Barrett, M.P., Brun, R., Gilbert, I.H., Hanau, S. **Selective Inhibition of *Trypanosoma brucei* 6-Phosphogluconate Dehydrogenase by High-Energy Intermediate and Transition-State Analogues.** J. Med. Chem., 2004, 47, 3427-3437.
49. Pasti, C., Rinaldi, E., Cervellati, C., Dallocchio, F., Hardre, R., Salmon, L., Hanau S. **Sugar Derivatives as New 6-Phosphogluconate Dehydrogenase Inhibitors Selective for the Parasite *Trypanosoma brucei.*** Bioorg. Med. Chem., 2003, 11, 1207-1214.
50. Barrett M. P, Phillips C, Adams M. J, Le Page R. W, **Overexpression in Escherichia coli and purification of the 6-Phosphogluconate Dehydrogenase of *Trypanosoma brucei.*** Protein Expr. Purif. 1994, 5, 44-49.
51. Horecker BL **Preparation and analysis of 6-phosphogluconate.** Methods Enzymol 1955, 3, 172-174.
52. Tashima Y & Yoshimura N **Control of rabbit liver fructose-1,6-diphosphatase activity by magnesium ions.** J Biochem 1975, 78, 1161-1169.
53. S. Hanau, K. Montin, H. Gilbert, M.P. Barrett and Dallocchio **Inhibitors of *Trypanosoma brucei* 6-Phosphogluconate Dehydrogenase,** Current Bioactive Compounds 2007, 3, 161-169.
54. Ruda GF, Alibu VP, Mitsos C, Bidet O, Kraiser M, Brun R, Barrett MP & Gilbert IH **Synthesis and biological evaluation of phosphate prodrugs of 4-phospho-D-erythronohydroxamic acid, an inhibitor of 6-phosphogluconate dehydrogenase.** ChemMedChem 2007, 2, 1169-1180.

55. Hanau S, Rippa M, Bertelli M, Dallocchio F & Barrett MP **6-Phosphogluconate dehydrogenase from *Trypanosoma brucei*. Kinetic analysis and inhibition by trypanoacidal drugs.** Eur J Biochem 1996, 240, 592-599.
56. I.R. McKinnon, L. Fall, A. Parody-Morreale, S. J. Gill, **A twin titration microcalorimeter for the study of biochemical reactions,** Anal Biochem. 1984, 139, 134-139.
57. T. Wiseman, S. Williston, J.F. Brandts, L.N. Lin, **Rapid measurement of binding constants and heats of binding using a new titration calorimeter**, Anal. Biochem. 1989,179, 131– 137.
58. E. Freire, O.L. Mayorga, M. Straume, **Isothermal titration calorimetry**, Anal. Chem. 1990, 62, 950A– 959A.
59. M. El Harrous, S.J. Gill, A. Parody-Morreale, **Description of a new Gill titration calorimeter for the study of biochemical reactions: I. Basic response of the instrument**, Meas. Sci. Technol. 1994, 5, 1065–1070.
60. M. El Harrous, O.L. Mayorga, A. Parody-Morreale, **Description of a new Gill titration calorimeter for the study of biochemical reactions:II. Operational characterization of the instrument**, Meas. Sci. Technol. 1994, 5, 1071– 1077.
61. A. Velazquez-Campoy, O. Lopez-Mayorga, M.A. Cabrerizo-Vilchez, **Development of an isothermal titration microcalorimetric system with digital control and dynamic power Peltier compensation: I. Description and basic performance**, Rev. Sci. Instrum. 2000, 71, 1824–1831.
62. A. Velazquez-Campoy, O. Lopez-Mayorga, M.A. Cabrerizo-Vilchez, **Development of an isothermal titration microcalorimetric system with digital control and dynamic power Peltier compensation: II. Characterization and operation mode. Myoglobin adsorption onto polymeric latex particles**, Rev. Sci. Instrum. 2000, 71, 1832– 1840.

63. A. Vela´zquez-Campoy, E. Freire, **Isothermal titration calorimetry: measuring intermolecular interactions**, in: R. Simpson (Ed.), Proteins and Proteomics: A Laboratory Manual, Cold Spring Harbor Laboratory Press, New York, 2003, pp. 882– 892.
64. A. Velazquez-Campoy, S.A. Leavitt, E. Freire, **Characterization of protein-protein interactions by isothermal titration calorimetry**, Methods Mol. Biol. 2004, 261, 35– 54.
65. Hanau S., Dallocchio F. and Rippa M. **NADPH activates a decarboxylation reaction catalyze by lamb liver 6-Phosphogluconate dehydrogenase.** Biochim. Biophys. Acta 1982, 1122, 273-277.
66. Lafont V, Armstrong AA, Ohtaka H, Kiso Y, Amzel LM & Freire E **Compensating enthalpic and entropic changes hinder binding affinity optimization.** Chem Biol Drug Des 2007, 69, 413–422.
67. Hwang CC, Berdis AJ, Karsten WE, Cleland WW & Cook PF **Oxidative decarboxylation of 6-phosphogluconate dehydrogenase proceeds by a stepwise mechanism with NADP and APADP as oxidants.** Biochemistry 1998, 37, 12596–12602.
68. Longo. L, Vanegas C. O, Patel M, Rosti V, Haiqing L, Waka J, Merghoub T, Pandolfi P, Notaro R, Manova K and Luzzatto L. **Maternally trasmitted severe glucose 6-phosphate dehydrogenase deficiency is an embryonic lethal** The EMBO J. 2002, 21, 4229-39.
69. Lei Li, Lei Zhang, and Paul F. Cook **Role of the S128, H186, and N187 Triad in Substrate Binding and Decarboxylation in the Sheep Liver 6-Phosphogluconate Dehydrogenase Reaction.** Biochemistry, 2006, 45, 12680-12686.
70. Edgcomb SP, Baker BM & Murphy KP **The energetics of phosphate binding to a protein complex.** Protein Sci 2000, 9, 927–933.
71. Rippa M. and Signorini M. **Methods enzimology** 41, 237-240.

72. Ashwell G, Hickman J. **Enzymatic formation of xylulose 5-phosphate from ribose 5-phosphate in spleen,** J Biol Chem. 1957, 226, 65-76.

73. Rippa M, Signorini M, Dallocchio F. **A role for the pyridine nitrogen of reduced triphosphopyridinenucleotide in an enzymatic catalysis,** FEBS Lett. 1973, 36, 148-50.

74. Hwang CC, Berdis AJ, Karsten WE, Cleland WW, Cook PF. **Oxidative decarboxylation of 6-phosphogluconate by 6-phosphogluconate dehydrogenase proceeds by a stepwise mechanism with NADP and APADP as oxidants,** Biochemistry. 1998, 37, 12596-12602.

75. Berdis AJ, Cook PF. **Overall kinetic mechanism of 6-phosphogluconate dehydrogenase from Candida utilis,** Biochemistry. 1993, 32, 2036-2040.

76. Rippa M, Signorini M, Dallocchio F. **A multiple role for the coenzyme in the mechanism of action of 6-phosphogluconate dehydrogenase. The oxidative decarbosylation of 2-deoxy-6-phosphogluconate,** J Biol Chem. 1973, 248, 4920-5.

77. W. Wallace Cleland **Measurement of Isotope Effects by the Equilibrium Perturbation Technique** Methods in enzymology vol. 64, part.B, 104-125.